Volume 7
Number 2
February 2020
Pages 303–626

Materials Horizons

rsc.li/materials-horizons

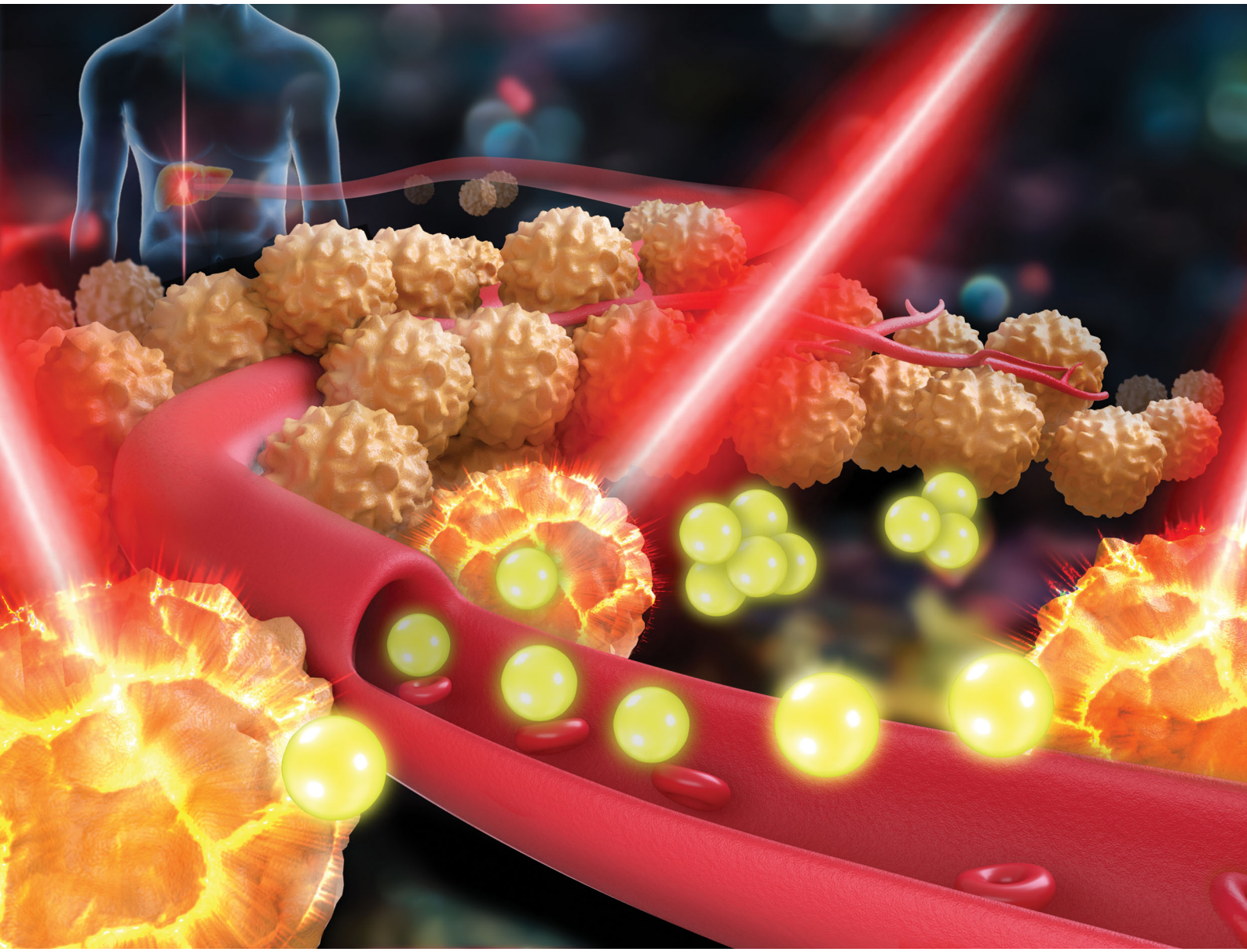

ISSN 2051-6347

ROYAL SOCIETY OF CHEMISTRY

REVIEW ARTICLE
Xiangxiang Jing, Yu Chen *et al.*
Catalytic chemistry of iron-free Fenton nanocatalysts for versatile radical nanotherapeutics

Materials Horizons

REVIEW

View Article Online
View Journal | View Issue

Cite this: *Mater. Horiz.*, 2020, 7, 317

Catalytic chemistry of iron-free Fenton nanocatalysts for versatile radical nanotherapeutics

Qiqing Chen,[a] Dayan Yang,[a] Luodan Yu,[b] Xiangxiang Jing*[a] and Yu Chen *[b]

The conversion of nontoxic agents into therapeutic species *in situ*, just within the disease microenvironment, is the ideal strategy because it can substantially enhance the therapeutic efficacy but mitigate the side effect to normal cells/tissues. The emerging nanocatalytic medicine based on the catalytic Fenton reaction can achieve this goal by triggering a disease-specific catalytic reaction to produce therapeutic reaction oxygen species. Traditional iron-based Fenton nanocatalysts are the dominant agents for triggering *in situ* reactions and radical nanotherapeutics, but they suffer from low reaction rate and narrow pH operation range, significantly hindering their further biomedical applications and clinical translation. Fortunately, the emergence of iron-free nanocatalysts provides alternative but highly efficient nanoplatforms for achieving desirable Fenton reaction-based nanocatalytic radical therapeutics. This comprehensive review discusses the very-recent progress on the elaborate design, rational construction, purpose-oriented multifunctionalization and catalytic property–performance relationship of iron-free Fenton nanocatalysts (*e.g.*, transition metal-based, precious-metal-based, nonmetal-based nanocatalysts and their composites) for versatile radical nanotherapeutics. The focus is particularly on the underlying catalytic chemistry and mechanism for endowing these iron-free nanocatalysts with unique/specific physicochemical properties for anticancer, antibacterial, antibiofilm and synergistic biomedical applications. Finally, we concentrate on the unresolved critical issues, current challenges and future development direction/prospects of these iron-free Fenton nanocatalysts for future clinical translations.

Received 2nd October 2019,
Accepted 14th November 2019

DOI: 10.1039/c9mh01565e

rsc.li/materials-horizons

1. Introduction

With the rapid social development, ever-increasing attention and great efforts have been devoted to the health of human beings, which have enabled the emergence of diverse theranostic modalities and protocols for combating various serious diseases. Nanotechnology-enabled nanomedicine has been regarded as the intriguing next-generation advanced medicine that might revolutionize disease theranostics to possibly achieve early diagnosis and efficient therapeutics of diseases.[1–8] Various novel therapeutic modalities have emerged, accompanied by the creation of abundant nanoplatforms with different nanostructures, compositions, biological effects and theranostic performances. These include the well-demonstrated and mostly explored photonic therapy (*e.g.*, photothermal or photodynamic therapy),[9–14] sono-triggered therapy (*e.g.*, sonodynamic therapy, high-intensity-focused ultrasound ablation),[15–18] magnetic hyperthermia,[19–22] nanomedicine-enabled targeted drug delivery,[23–27] nanomedicine-enhanced gene therapy,[28–30] and some synergistic therapeutics.[31–33] In particular, the emergence of "nanocatalytic medicine" fully utilizes the physicochemical properties (*e.g.*, catalytic activity, energy-converting property) and biological effects (*e.g.*, enzyme-mimicking behavior) of nanoparticles to achieve disease-specific biological imaging and versatile nanotherapeutics.[2,34,35]

Reactive oxygen species (ROS)-based therapeutic biomedicine involves the generation of diverse ROS by either exogenous triggering or endogenous reaction, including hydroxyl radicals ($^{\bullet}OH$), singlet oxygen ($^{1}O_2$), superoxide anions ($^{\bullet}O_2^{-}$), H_2O_2, *etc.*[4,36] These ROS can induce therapeutic effects such as killing cancer cells or antibacterial activity. Among the diverse ROS-based nanotherapeutics, the catalytic Fenton reaction-induced ROS generation belongs to the emerging concept of "nanocatalytic medicine".[37–39] The intrinsic mechanism of the catalytic Fenton reaction is the conversion of hydrogen peroxide (H_2O_2) into hydroxyl ($^{\bullet}OH$) radicals with the assistance of Fenton catalysts under acidic conditions.[40–44] Fenton-like reaction-based nanocatalytic therapy based on radical production is highly preferable for tumor treatment. The tumor-overexpressed H_2O_2 by superoxide dismutase overexpression in the range of 100 μM^{-1} mM acts as the reactant for the Fenton reaction.[45–47] The acidity makes it a preferable reaction[48] since it matches well with the mildly acidic

[a] *Department of Ultrasound, Hainan General Hospital, Haikou, 570311, P. R. China. E-mail: ljjxx2000@126.com*
[b] *State Key Lab of High Performance Ceramics and Superfine Microstructure, Shanghai Institute of Ceramics, Chinese Academy of Sciences, Shanghai, 200050, P. R. China. E-mail: chenyu@mail.sic.ac.cn*

tumor microenvironment due to the rapid glycolytic metabolism of tumor cells.[49] Therefore, such a Fenton-like reaction is highly tumor-specific, which is fortunately hard to trigger in normal cells/tissues, thus guaranteeing much less harm to normal cells/tissues and therefore high therapeutic biosafety. Compared to traditional therapeutic modalities such as chemotherapy and radiation, such a Fenton-based nanotherapeutic modality only exerts the therapeutic functionality in tumor tissue because of the tumor specificity, which means that the therapeutic efficiency is high while the therapeutic side effects are low, guaranteeing its high potential for further clinical translation.

Iron (Fe)-based homogeneous or heterogeneous catalysts are the most explored catalytic systems for triggering the Fenton reaction. Diverse Fe-based nanocatalysts have been fabricated for achieving Fenton reaction-based nanocatalytic therapies for cancer treatments, including Fe_3O_4 nanoparticles,[50–52] Fe_5C_2 nanoparticles,[53] FeS nanosheets,[54] and some Fe-based nanocomposites.[55] These iron-based nanocatalysts have been demonstrated to be highly effective in biofilm disruption.[56–58] Although Fe-based nanomedicines are effective in inducing ROS generation for radical nanotherapeutics, the Fe(II)-catalyzed Fenton reaction still suffers two critical issues. On the one hand, strongly acidic conditions are required for the Fe(II)-catalyzed Fenton reaction, which is difficult to achieve in the mildly acidic tumor microenvironment.[59] On the other hand, the reaction rate of the Fe(II)-catalyzed Fenton reaction is relatively low ($\sim 63\ M^{-1}\ s^{-1}$), hindering the production of sufficient ROS for therapeutic applications.[60] Therefore, increasing attention has been directed toward exploring the alternatives to Fe-based nanocatalysts in Fenton reaction-based radical nanotherapeutics, which has become one of the fastest research frontiers in nanomedicine and nanobiotechnology.

It has been demonstrated that some metal-based nanocatalysts are more preferable as the catalysts for the catalytic Fenton reaction.[42,49,61] For instance, compared to iron-based nanocatalysts, Cu-involved nanocatalysts can exert catalytic Fenton activity on the Fenton reaction in a much broader pH range.[62,63] Cu(II) is also more easily reduced to Cu(I) in the cycle of Cu(II)/Cu(I), as compared to Fe(III) to Fe(II) in the cycle of Fe(III)/Fe(II), thus enabling a higher reaction rate ($1 \times 10^4\ M^{-1}\ s^{-1}$, ~160-fold higher as compared to Fe(II)) in the Fenton reaction to transform H_2O_2 into hydroxyl radicals.[49,64–66] Therefore, versatile Cu-based nanocatalysts have been developed for Fenton reaction-based tumor therapy, including copper peroxide, CuS, CuSe, Cu–cysteine mercaptide, copper hydroxyphosphate, *etc.* In addition, the abundant compositions and some specific physicochemical properties of iron-free Fenton nanocatalysts endow them with unique functionality for radical nanotherapeutics, such as Fenton reaction-based synergistic therapy including the integration with photothermal ablation, photodynamic therapy (PDT) and chemotherapy.

In addition to Cu-based nanocatalysts as the efficient alternatives to the traditional iron-based Fenton nanoagents for nanocatalytic tumor therapy, a variety of iron-free nanocatalysts has very recently been introduced into the catalytic reaction for versatile biomedical applications. In this review, we discuss the intrinsic catalytic chemistry of iron-free nanocatalysts for satisfying the versatile radical nanotherapeutics, especially their unique physicochemical properties and catalytic performance for triggering the catalytic Fenton reaction *in situ* to produce ROS and subsequently induce desirable therapeutic

Xiangxiang Jing

Prof. Xiangxiang Jing received her Bachelor's and Master's degree from Shanxi Medical University and PhD from Chongqing Medical University. She is now the chief physician at Hainan General Hospital. Her research includes clinical ultrasound imaging and ultrasonic contrast agents for targeted molecular imaging and therapy, and the development of nanobiotechnology-based disease diagnosis and therapy, especially for cancer diagnosis and therapy. She has published over 20 scientific papers.

Yu Chen

Prof. Yu Chen received his Bachelor's degree at Nanjing Tech University and PhD at Shanghai Institute of Ceramics, Chinese Academy of Sciences (SICCAS). He is now a full professor at SICCAS. His research focuses on Materdicine (interdiscipline of materials and medicine), which includes the design, synthesis and biomedical applications of zero-dimensional mesoporous biomaterials (mesoporous silica/organosilica), two-dimensional biomaterials (graphene, metal oxides, TMDCs, MXenes and Xenes) and 3D-printing scaffolds, including nanocarriers for drug/gene delivery, molecular probes for molecular imaging, and nanoagents for nanocatalytic therapy, energy-conversion nanotherapy and in situ localized disease therapy. He has published more than 180 scientific papers in the Materdicine field with a total citation of more than 12 000 times (h-index: 59). He was recognized as a Highly Cited Researcher for 2018 by Clarivate Analytics, Web of Science.

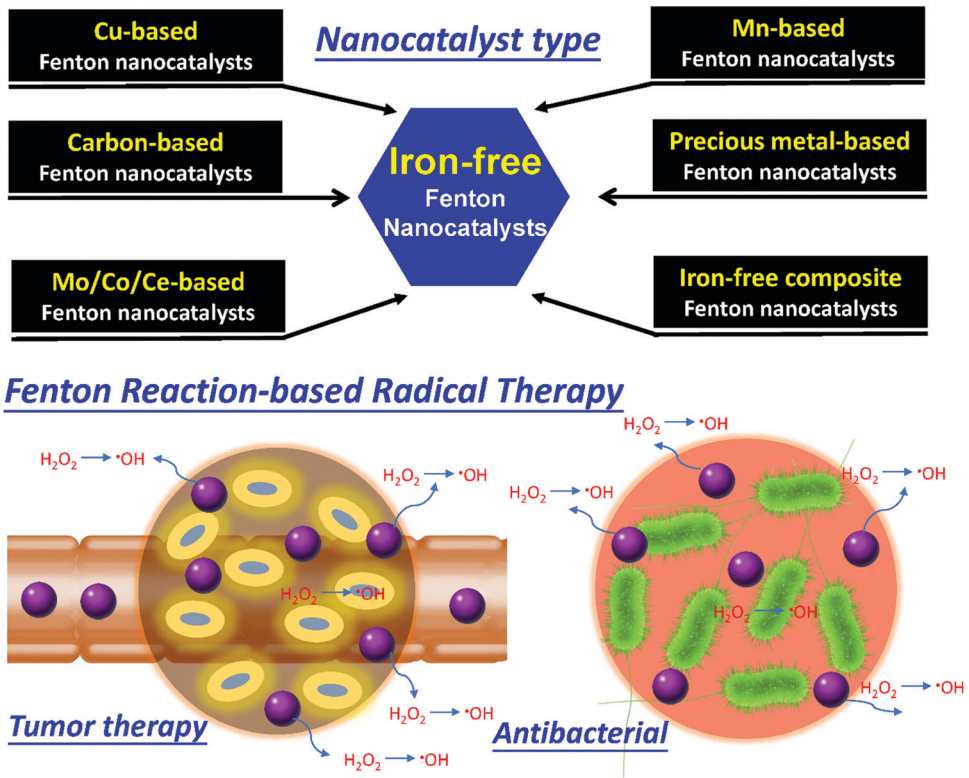

Fig. 1 Scheme showing the types of iron-free Fenton nanocatalysts and specific Fenton reaction-based radical nanotherapeutics such as tumor therapy and antibacterial application.

effects (Fig. 1). Versatile iron-free nanocatalysts are involved in this review, among which transition metals and precious metals-based nanocatalysts play the dominant roles, with some examples of carbon-based nonmetal nanocatalysts. From the viewpoint of catalytic chemistry, the underlying catalytic mechanism of the Fenton reaction in the disease microenvironment is also discussed, accompanied by the specific biomedical applications in cancer therapy, antibacterial activity and antibiofilm formation. The integration of Fenton reaction-based oxidative therapy with other therapeutic modalities is further discussed through the elaborate design of multifunctional iron-free Fenton nanocatalysts. The specific features and advantages of this therapeutic modality, as enabled by the nanocatalytic Fenton reaction, are compared to other traditional therapeutic protocols, in addition to the advantages of iron-free nanocatalysts as compared to traditional Fe-based Fenton nanocatalysts. Finally, we discuss the state-of-the-art challenges, unresolved critical issues and future prospects of this catalytic therapeutic modality as enabled by iron-free nanocatalysts for further potential clinical translation.

2. Cu-Based Fenton nanocatalysts

Copper (Cu) plays a significant role in the redox reactions of natural enzymes where Cu is present with the integration with proteins or other ligands.[67–70] Free Cu ions are toxic and they cannot be directly used in the body. For the catalytic Fenton reaction, Cu-involved nanocatalysts are featured with three distinctive advantages for tumor therapy. First, the Cu-triggered Fenton reaction can be operated in a broad pH range. Second, Cu(II) is vulnerable to reduction to Cu(I). Third, the hypoxic tumor microenvironment could protect the oxidation of Cu(I) by oxygen. Therefore, versatile Cu-based Fenton nanocatalysts have been developed for nanotherapeutics, including copper peroxide, CuS, CuSe, Cu–cysteine mercaptide, copper hydroxyphosphate, *etc.*, which have been discussed in detail as the paradigms in this section.

Based on the high coordination capability of Cu ions with sulfhydryl-group-containing ligands, a Cu-containing nanoformulation of Cu–cysteine mercaptide (Cu–Cys) was constructed for the Cu-catalyzed Fenton reaction and the subsequent nanocatalytic tumor radical therapy.[71] Based on much higher GSH levels in tumor cells as compared to normal cells, these Cu–Cys nanoparticles were easily reduced by intracellular GSH to transform Cu^{2+} into Cu^{+}. This process also consumed GSH to modulate the tumor-reducing microenvironment. The tumor-overexpressed H_2O_2 was then transformed into highly toxic hydroxyl radicals by the Cu^{+}-catalyzed Fenton-like reaction (Fig. 2a). Comparatively, in normal cells, the low-level GSH would not reduce Cu^{2+} into Cu^{+}, and the low-expression H_2O_2 would also not be converted into ROS, enabling the high therapeutic biosafety of these Cu–Cys nanocatalysts. On administering equivalent doses (5 mg kg^{-1}) of Cu–Cys nanoparticles and the typical chemotherapeutic drug doxorubicin (DOX) into NOD-SCID immune-deficient mice bearing MCF-7R orthotopic xenografts (Fig. 2b), there was a substantially

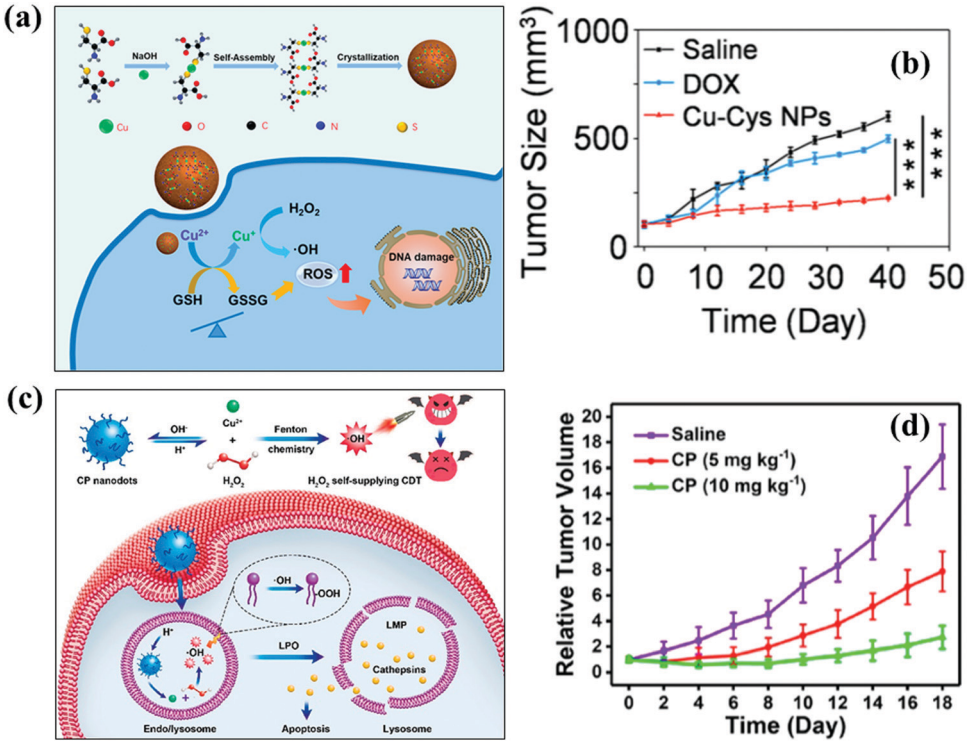

Fig. 2 (a) Schematic illustration of the construction of Cu–Cys nanoparticles and their specific catalytic properties in triggering the Fenton-like reaction to produce toxic hydroxyl radicals and subsequently inducing cancer-cell apoptosis. (b) *In vivo* tumor-size changes by the treatments of either the chemotherapeutic drug DOX or Cu–Cys nanocatalysts.[71] Copyright 2019, American Chemical Society. (c) Scheme showing the fabrication of CP nanodots for stepwise H_2O_2 production and subsequent Cu-catalyzed Fenton reaction, inducing the intracellular generation of hydroxyl radicals to kill the tumor cells by lysosomal lipid peroxidation. (d) Tumor-volume changes after the administration of CP at different doses (5 and 10 mg kg^{-1}).[72] Copyright 2019, American Chemical Society.

enhanced tumor-suppression effect in the nanoparticles group (inhibition rate of 72.3%) as compared to the DOX group (inhibition rate of 17.1%), accompanied by the high histocompatibility of this nanocatalytic therapeutic process.[71]

For the nanocatalyst-enhanced Fenton reaction, the H_2O_2 amount, as the reactant, determines the reaction rate/degree and final ROS production. Although the H_2O_2 level in tumor cells is higher than that of normal cells, the endogenous H_2O_2 amount is typically not high enough to achieve the desired therapeutic outcome. To solve this critical issue, copper peroxide (CP) nanodots were rationally constructed for catalyzing the H_2O_2-self-supplying Fenton reaction to achieve nanocatalytic radical therapy (Fig. 2c).[72] These CP nanodots were fabricated by coordination between H_2O_2 and Cu^{2+} based on the assistance of hydroxide ions, where poly(vinylpyrrolidone) (PVP) was used for surface modification. CP nanodots produced H_2O_2 under acidic conditions to provide the reactants for the subsequent Cu-catalyzed Fenton reaction and then produce hydroxyl radicals, which further induced the tumor-cell death by lysosomal lipid peroxidation. By the intravenous administration of these PVP-coated CP nanodots into U87MG tumor-bearing mice, the tumor growth was substantially suppressed in a dose-dependent manner (Fig. 2d). This work provides a paradigm for the construction of H_2O_2 self-supplying iron-free nanocatalysts for efficiently triggering the intracellular Fenton reaction and radical nanotherapeutics.

Similarly, Cu-doped superoxide dismutase (SOD)-encapsulated $CaCO_3$-mineralized nanoparticles were constructed for the pH-responsive release of loaded SOD and Cu ions.[73] SOD induced the generation of H_2O_2, providing the reactant, which was further catalyzed by the released Cu ions for hydroxyl radical production and subsequent oxidative-stress augmentation to induce the cancer-cell toxicity with negligible toxicity to normal NIH3T2 and HEK293 cells. The loading of glucose oxidase (GOx) onto the surface of 2D Cu–TCPP nanosheets also triggered the sequential nanocatalytic reaction for antibacterial use, where GOx catalyzed glucose to produce gluconic acid and H_2O_2. The produced H_2O_2 acted as the Fenton reactant and gluconic acid decreased the local pH to accelerate the reaction rate.[74]

The introduction of external energy input could further enhance the Fenton reaction efficiency as catalyzed by iron-free nanocatalysts. As a paradigm, copper hydroxyphosphate nanocrystals ($Cu_2(OH)PO_4$ NCs) with size of 5 ± 2 nm were constructed for Fenton-like nanocatalytic therapy, which was triggered by X-ray irradiation to convert Cu^{II} sites into Cu^{I} sites.[75] The converted Cu^{I} showed enhanced catalytic performance on transforming endogenous tumor-overexpressed H_2O_2 into hydroxyl radicals (Fig. 3a). Based on the photoelectric effect, the X-ray photons interacted with the atoms in the lattices of $Cu_2(OH)PO_4$ NCs to concomitantly induce the avalanche of

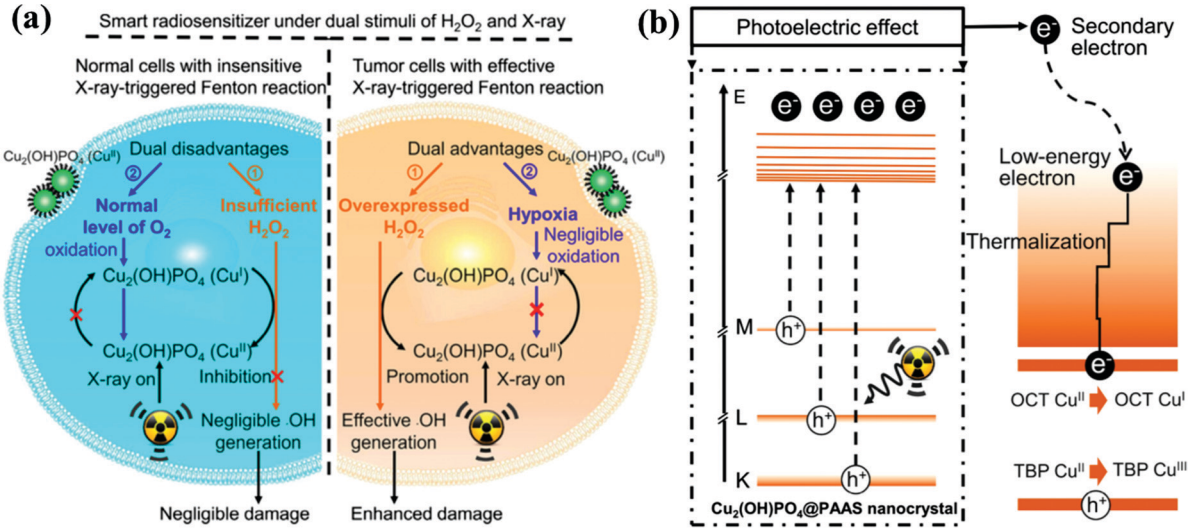

Fig. 3 (a) Schematic illustration of the as-constructed $Cu_2(OH)PO_4$@PAAS nanocrystals for achieving an X-ray-triggered Fenton-like reaction just within the tumor microenvironment rather than the normal cells/tissue. (b) The scheme of the underlying mechanism for the generation of Cu^{I} sites in $Cu_2(OH)PO_4$@PAAS nanocrystals by exogenous X-ray irradiation.[75] Copyright 2019, American Chemical Society.

low-energy electrons and holes, which was separate from high-energy electrons and holes and was unable to trigger the subsequent ionization (Fig. 3b). These post-generated low-energy electrons and holes realized the respective generation of OCT-Cu^{I} and TBP-Cu^{III} sites by being thermalized in the OCT-Cu^{II} and TBP-Cu^{II} sites. Importantly, such a Cu-triggered Fenton reaction was difficult to trigger in normal cells/tissues because of the oxygen-rich environment and much lower H_2O_2 level as compared to the tumor tissue. Based on the high tissue-penetrating depth of X-rays, this strategy is highly promising for the treatment of deep-seated tumors by triggering the Cu-catalyzed Fenton reaction *in situ*.[75]

Extensive studies have shown that some Cu-based nanoparticles, such as CuS, are featured with high photothermal-conversion properties for photonic tumor hyperthermia.[79–83] Therefore, it is reasonably anticipated that such a photothermally-induced local temperature elevation could accelerate the Cu-catalyzed Fenton reaction because this catalytic reaction is temperature-dependent. As such, ultrasmall $Cu_{2-x}S$ nanoparticles, with particle size of less than 5 nm, were fabricated with surface PEGylation for photothermally-enhanced catalytic Fenton reaction and synergistic tumor therapy (Fig. 4a).[76] The co-existence of Cu^{2+} and Cu^{+} was more preferable for producing hydroxyl (•OH) radicals, and the NIR irradiation at the second biological window (NIR-II) elevated the local temperature to further accelerate the ROS generation, along with photoacoustic (PA) imaging guidance and monitoring. The synergy was demonstrated not only in inducing cancer-cell death *in vitro*, but also in inhibiting tumor growth *in vivo* against 4T1 tumor xenografts on nude mice. Cu^{+} was released from polyvinylpyrrolidone-modified CuS nanocrystals with a highly active (102) surface to trigger the Fenton-like reaction for radical-based tumor nanotherapeutics, which was also responsive to the endogenous tumor microenvironment and NIR laser irradiation.[84] Similarly, Cu_2Se hollow nanocubes (Cu_2Se HNCs) were constructed by an anion exchange protocol with pre-synthesized Cu_2O nanocubes as the hard template (Fig. 4b).[77] These Cu_2Se HNCs exhibited similar performance to the aforementioned $Cu_{2-x}S$–PEG nanoparticles, by which the NIR-II-activated photothermal-enhanced nanocatalytic efficacy of the Fenton reaction was achieved for synergistic ROS production-induced cancer-cell death and photothermal cancer ablation (Fig. 4c).

Most Cu-based nanocatalysts for the Fenton reaction are based on inorganic Cu-involved nanosystems that might suffer from low biodegradability *in vivo*. Comparatively, Cu-composed organic nanoparticles could potentially solve this biodegradation issue. For instance, Cu^{2+}-mediated protein self-assemblies (designated as C-m-ABs) were constructed by the combination of Cu ions and the photosensitizer indocyanine green (ICG).[78] The intracellular GSH reduced Cu^{2+} to Cu^{+}, which caused the catalysts for the Fenton reaction to produce •OH. Importantly, the light irradiation enhanced the •OH production efficacy, enabling C-m-ABs to act as a photo-Fenton-like nanocatalyst (Fig. 4d). C-m-ABs were also effective in converting H_2O_2 into O_2 to modulate the tumor hypoxia and enhance the photodynamic performance of the loaded ICG photosensitizer.

It is well-known that Cu^{+} is more preferable and catalytically active for triggering the Fenton reaction to produce ROS. We recently designed a nanocarrier-based Cu^{2+}-to-Cu^{+} conversion reaction for Fenton reaction-enhanced chemotherapy. Disulfiram (DSF) has been approved by the US Food and Drug Administration (FDA) for the treatment of alcohol dependence, and is also highly effective in cancer chemotherapy with Cu-dependent cytotoxicity.[87–91] We designed PEGylated Cu^{2+}-doped hollow mesoporous silica nanoparticles (PEG/Cu-HMSNs) for tumor-specific Cu^{2+} release to enhance the chemotherapeutic efficacy of DSF by Fenton reaction-induced ROS generation (Fig. 5a).[85] The released Cu^{2+} ions were easily coordinated with

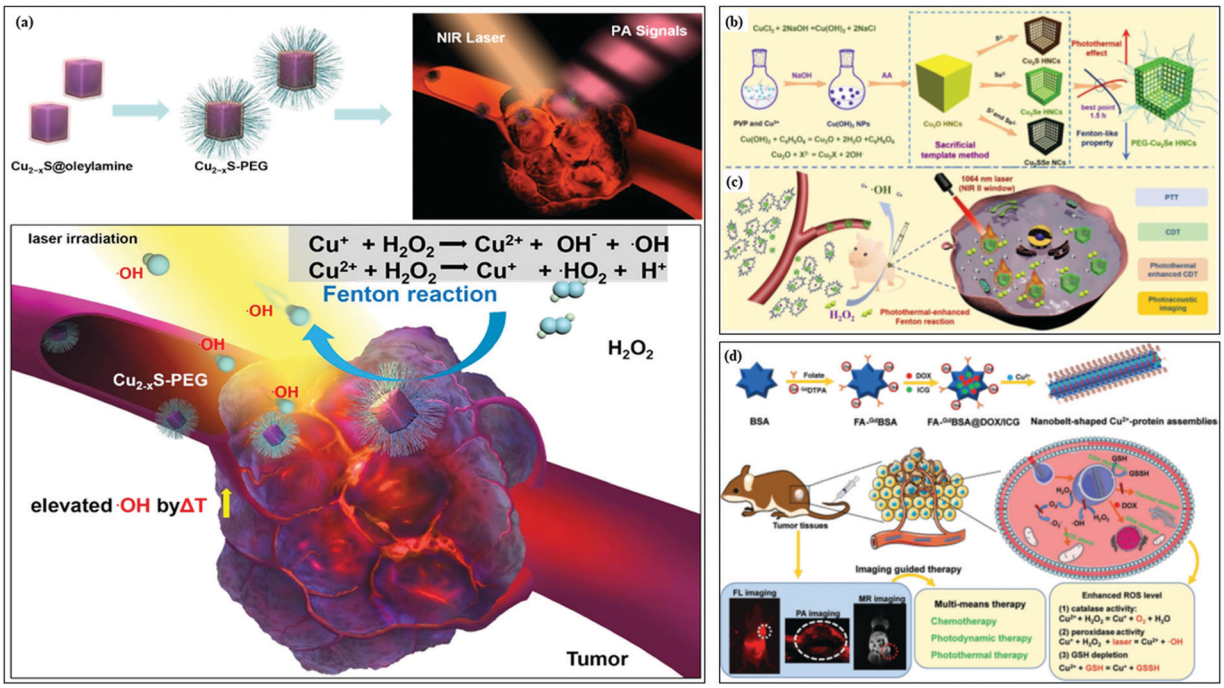

Fig. 4 (a) Schematic illustration of the construction of $Cu_{2-x}S$–PEG nanocatalysts for the photothermally-enhanced Fenton reaction-induced nanocatalytic tumor therapy with PA-imaging guidance.[76] Copyright 2019, Elsevier. (b) Schematic illustration of the fabrication mechanism of PEG–Cu_2Se hollow nanocubes (Cu_2Se HCNs) for (c) synergistic photothermal ablation and hyperthermia-enhanced Fenton reaction for nanocatalytic tumor therapy.[77] Copyright 2019, American Chemical Society. (d) Schematic illustration of the construction of nanobelt-shaped Cu^{2+}–protein assemblies for synergistic cancer therapy, including photo-triggered enhanced ROS production by the Cu-catalyzed Fenton reaction and photodynamic procedure, accompanied by PA and MR imaging guidance and monitoring performance.[78] Copyright 2019, John Wiley and Sons.

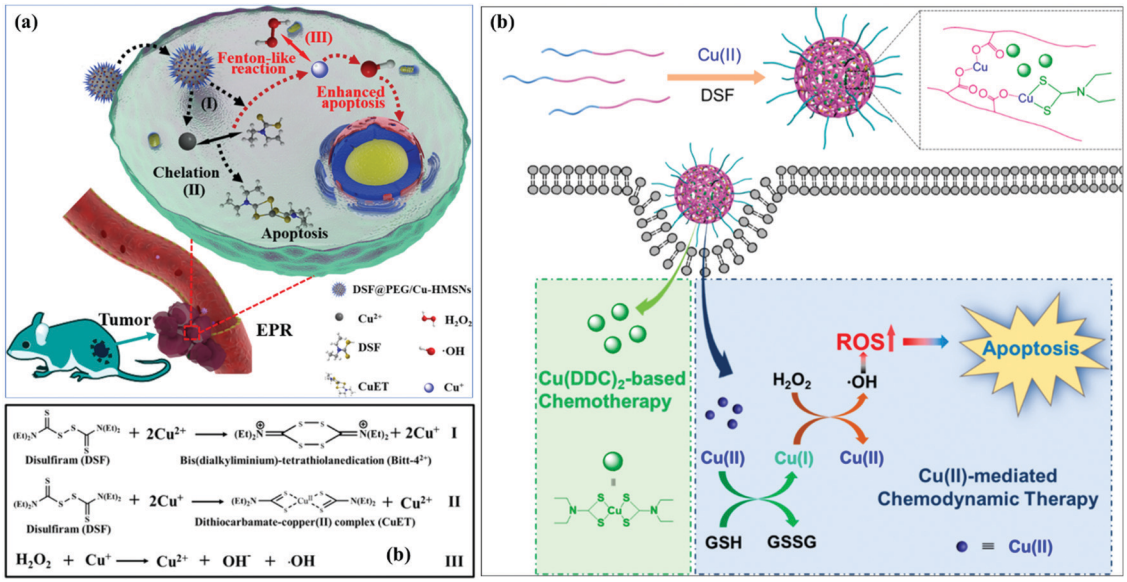

Fig. 5 (a) Schematic illustration of the intracellular therapeutic procedure of DSF@PEG/Cu-HMSNs by the synergistic Cu-catalyzed Fenton reaction-induced ROS generation and CuET formed *in situ*.[85] Copyright 2019, American Chemical Society. (b) Schematic illustration of the construction of Cu(II)/DDC-loaded nanodrugs for intracellular delivery and synergistic chemotherapy and Cu(II)-triggered Fenton reaction-induced radical therapy.[86] Copyright 2019, American Chemical Society.

DSF to form Cu–dithiocarbamate complexes (CuETs), which were highly toxic to cancer cells. The DSF/Cu^{2+}-chelating process generated an intermediate product of Cu^+ ions that could efficiently trigger the Fenton-reaction under the specific tumor microenvironment of overexpressed H_2O_2 and mild acidity. This process produced highly toxic hydroxyl ($^{\bullet}OH$) radicals for synergistically

enhancing the cytotoxicity of CuETs, achieving high tumor-inhibition efficacy. This design principle also provides a paradigm for designing tumor-specific chemotherapy with "nontoxicity-to-toxicity" translation performance. Similarly, Cu(II) diethyldithiocarbamate ($Cu(DDC)_2$) was loaded into poly(ethylene glycol)-*b*-poly(ester-carbonate) nanoparticles for achieving a combination therapy that was based on $Cu(DDC)_2$-induced chemotherapy and the residual Cu(II)-initialized Fenton reaction-induced radical ($^{\bullet}OH$) oxidative therapy (Fig. 5b).[86] The low dose of the Cu(II)/DDC-loaded nanomedicine augmented the anticancer outcome as demonstrated both *in vitro* and *in vivo*.

In addition to the interaction of released Cu from mesoporous silica framework with DSF for synergistic chemotherapy and radical therapy, the simultaneous incorporation of Cu and Fe components into the framework of mesoporous silica was demonstrated to trigger the Fenton reaction and produce hydroxyl radicals for enhancing the therapeutic efficacy of loaded traditional anticancer drug (doxorubicin, DOX).[92] As an alternative to the combination of Cu-catalyzed Fenton reaction-induced radical therapy with chemotherapy, a Cu(I)-based MOF acted as the Fenton nanoagent for generating hydroxyl radicals to enhance the photodynamic efficacy in combating cancer.[93] The integration of Cu^{2+} and graphitic carbon nitride (g-C_3N_4) enabled the construction of a composite photosensitive nanocatalyst with dual ROS-generation capability with depletion performance of intracellular GSH levels based on the Cu^{2+}-catalyzed Fenton-like reaction and photo-activated photodynamic ROS generation.[94] Similarly, the GSH-depletion capability was also achieved on two-dimensional ultrathin Cu–TCPP nanosheets to enhance ROS-based radical-generation efficacy.[95]

The Cu-catalyzed Fenton reaction-based radical therapeutic process could enhance the therapeutic outcome of immunotherapy, which originated from several examples of nanomedicine-augmented immunotherapy.[98–101] On this ground, Cu-clusters and porphyrin-based tetracarboxylic acid were assembled to form nanoscale nMOF for the combination of Cu^{2+}-triggered catalytic reaction-based chemodynamic therapy, light-triggered photodynamic therapy (PDT) and checkpoint blockade immunotherapy (Fig. 6a).[96] These nanoscale nMOFs degraded in acidic conditions to release Cu^{2+} and porphyrin. On the one hand, the released Cu^{2+} produced hydroxyl radicals by disturbing the metabolism of estradiol and potentially the Fenton-like chemical reaction. On the other hand, the released porphyrin acted as a photosensitizer for the photodynamic generation of single oxygen ($^1O_2$). The combined Cu^{2+}-triggered chemodynamic therapy and porphyrin-based PDT destroyed the primary tumors and subsequently released the tumor antigens. The further injection of anti-PD-L1 antibody induced the efficient suppression of distant tumors by the abscopal effect, which was demonstrated in a melanoma mouse model. This work provides the paradigm for the rational combination of Cu^{2+}-trigged radical therapy with checkpoint blockade immunotherapy for the efficient treatment of both primary and distant tumors.[96]

In addition, based on the desirable catalytic performance of Cu ions for the Fenton reaction, these Cu^{2+} ions were directly incorporated into the framework of organic–inorganic hybrid dendritic mesoporous organosilica nanoparticles (Cu-DMONs).[97] The framework-incorporated Cu^{2+} ions acted as the Fenton reagents to trigger ROS production ($^{\bullet}OH$) *in situ*, and the framework-hybridized tetrasulfide groups consumed the antioxidant glutathione (GSH) for radical protection (Fig. 6b). Combined with doxorubicin (DOX)-based chemotherapy, these DOX-loaded Cu-DMONs with high oxidative stress-inducing performance were demonstrated to possess high immune-adjuvant activity, which induced the maturation of antigen-presenting cells and the secretion of proinflammatory cytokines. Therefore, they were combined with immune checkpoint blockades (PD-L1) to achieve enhanced and synergistic chemo-immunotherapeutic efficacy, where not only the growth of primary tumors was substantially inhibited, but the growth of non-treated distant tumors was also significantly inhibited because of the induced high immunotherapeutic effect.[97]

3. Mn-Based Fenton nanocatalysts

Manganese (Mn) is one of the trace elements found in the human body and manganese element-involved nanosystems have recently been extensively explored in theranostic nanomedicine. Mn-Based nanoparticles in the form of metal oxides or nanocomposites are mostly developed as contrast agents for T_1-weighted contrast-enhanced magnetic resonance imaging (MRI) based on the paramagnetic nature of the Mn components.[102–105] These nanosystems have also been demonstrated to be effective in drug delivery,[106,107] gene transfection,[108] inducing ferroptosis[109] and photonic hyperthermia.[110] In addition, manganese oxides (MnO_x) could act as catalase-mimicking nanoenzymes to convert tumor-overexpressed hydrogen peroxide into oxygen, which could effectively alleviate tumor hypoxia to enhance the therapeutic efficacy of chemotherapy,[111] sonodynamic therapy,[15] photodynamic therapy[112–114] and radiotherapy.[115,116] Importantly, the released manganese ions from Mn-based nanosystems could act as the Fenton agents for catalyzing H_2O_2 into hydroxyl radicals in the presence of bicarbonate (HCO_3^-).[117]

The MnO_2-catalyzed Fenton reaction was achieved by constructing MS@MnO_2 nanoparticles *via* the direct reaction of thiol-functionalized mesoporous silica (MS) with permanganate, which coated a MnO_2 layer onto the surface of MS nanoparticles.[117] After endocytosis into cancer cells, the MnO_2 shell reacted with intracellular glutathione (GSH) to release Mn^{2+} and produce glutathione disulfide (GSSG). The post-generated Mn^{2+} triggered a Fenton-like chemical reaction by converting endogenous H_2O_2 into hydroxyl radicals with the assistance of bicarbonate (HCO_3^-), which was indispensable for triggering the Mn^{2+}-catalyzed Fenton-like reaction (Fig. 7a and b). Such a process could also deplete intracellular GSH to avoid $^{\bullet}OH$ consumption. Through the intravenous administration of PEGylated MS@MnO_2 nanocatalysts into U87MG tumor-bearing mice, the tumor growth was substantially inhibited (Fig. 7c) as

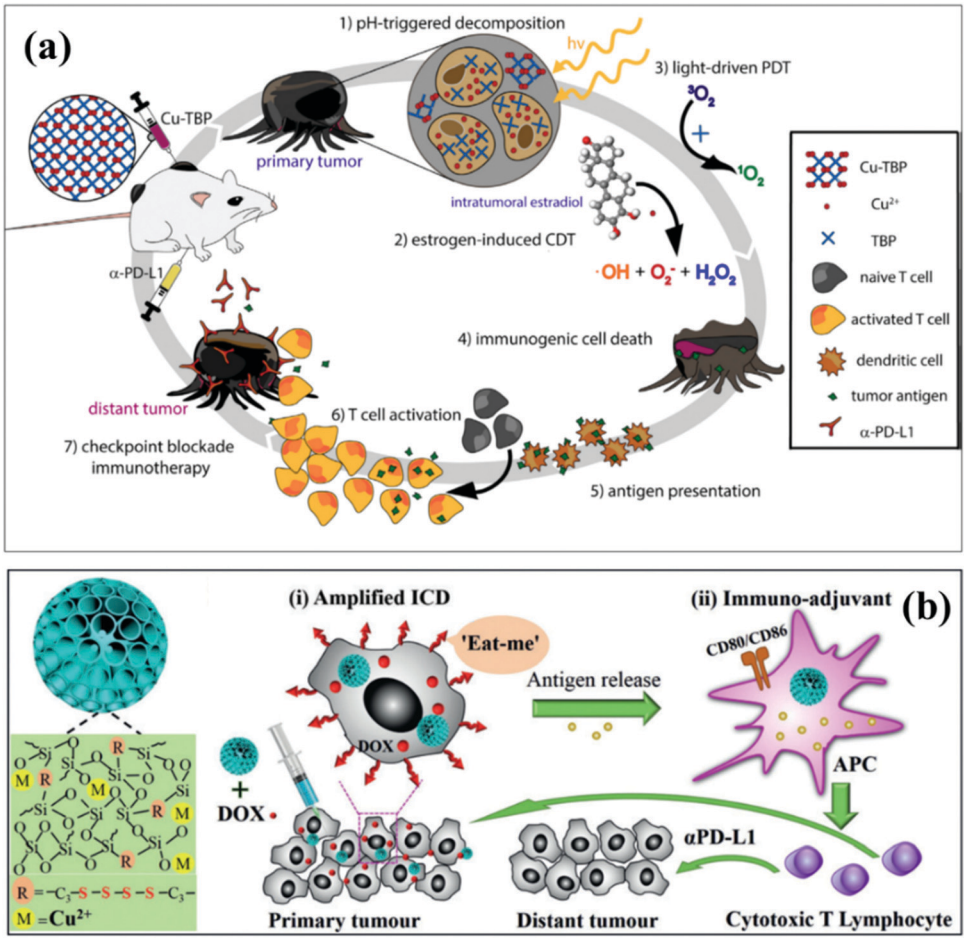

Fig. 6 (a) Schematic illustration of the combinatorial therapy based on nMOF-based/Cu^{2+}-triggered chemodynamic therapy, light-driven photodynamic therapy and checkpoint blockade immunotherapy.[96] Copyright 2019, Elsevier. (b) Schematic illustration of the microstructure and composition of organic–inorganic hybrid mesoporous organosilica nanoparticles with Cu^{2+} incorporated within the framework, and the synergistic Fenton reaction-induced ROS generation for enhancing DOX chemotherapy and acting as the immune adjuvants to induce the immune-cell maturation. This effect was further integrated with PD-L1 antibody-based immune checkpoint blockages, achieving effective suppression of both primary tumors and non-treated distant tumors.[97] Copyright 2018, John Wiley and Sons.

contributed by the Fenton reaction-induced elevation of oxidative stress for inducing cancer-cell apoptosis.[117]

To further augment the therapeutic efficacy, biodegradable copper/manganese silicate nanoparticles (CMSNs) were fabricated as multifunctional Fenton nanocatalysts for achieving tumor microenvironment-responsive synergistic PDT and nanocatalytic tumor therapy (Fig. 7d).[118] The surface of CMSNs was coated with an MCF-7 cancer-cell membrane (mCMSNs) to endow these nanocatalysts with homotypic-targeting capability. The copper–silica component contributed to the PDT-induced $^1O_2$ production, which was further enhanced by GSH depletion and tumor hypoxia relief because of the reaction between GSH and the framework of CMSNs. Such a reaction also induced the release of Cu^{2+} and Mn^{2+} ions to react with tumor-overexpressed H_2O_2 by a Fenton-like reaction mechanism with HCO_3^- assistance. Based on the targeting capability and enhanced catalytic performance, these mCMSNs substantially inhibited the tumor growth of MCF-7 tumor-bearing nude mice after intravenous administration.

For Mn-catalytic Fenton reaction-based synergistic tumor therapy, a MnO_2-coated $NaYF_4$:30%Yb,0.5%Tm@$NaYF_4$ upconversion hybrid nanocomposite (UCMn) was constructed, followed by conjugation with a *cis*-platinum prodrug (UCMnPt) and PEG for multiple biological imaging-guided synergistic cancer treatments (Fig. 8).[119] These UCMnPt featured several unique composition-dependent characteristics. First, the MnO_2 component reacted with intracellular GSH to release Mn^{2+}, which also depleted GSH for hindering the scavenging potential of GSH towards ROS such as hydroxyl radicals ($^{\bullet}OH$). Second, the *cis*-platinum prodrug acted as the chemotherapeutic drug to kill the cancer cells and generated H_2O_2 during a series of biological procedures, which provided the reactants for the Fenton reaction. Third, the released Mn^{2+} exerted catalytic functionality to trigger an intracellular Fenton reaction with both sufficient H_2O_2 reactant and chemotherapy synergy. As expected, the synergistic inhibition effect was achieved against HepG2 tumors on mice after intravenous administration of these UCMnPt nanocatalysts. It is noted that

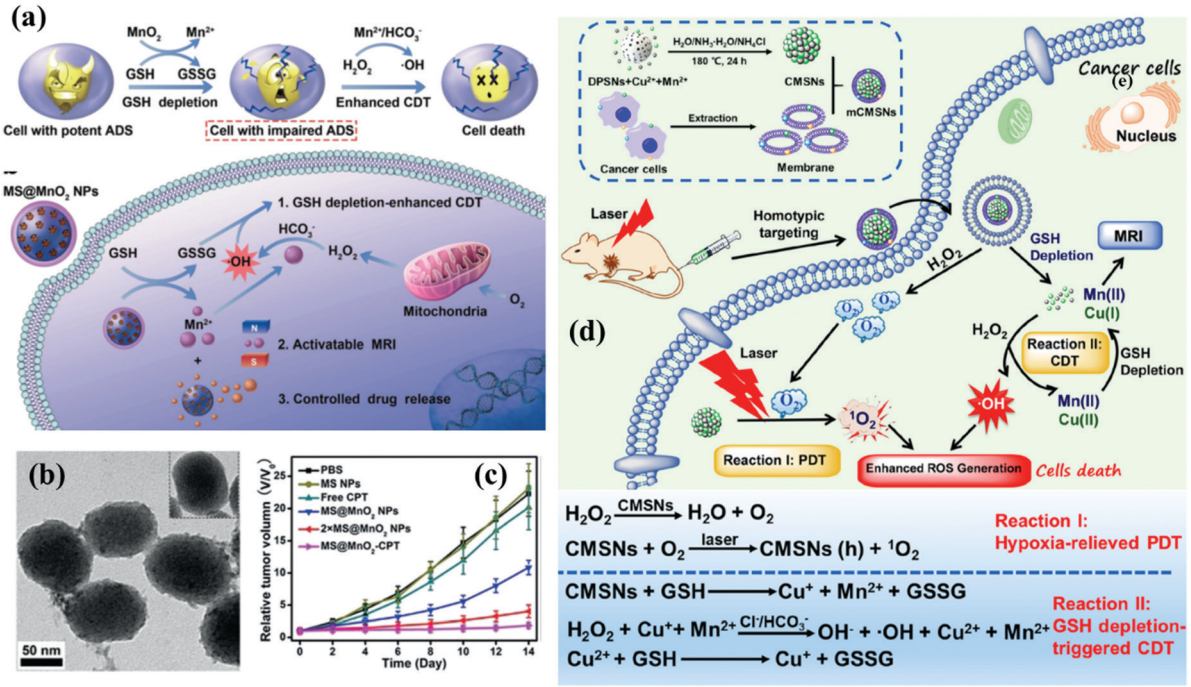

Fig. 7 (a) Schematic illustration of the underlying mechanism of the MnO_2-catalyzed Fenton reaction for hydroxyl radical production and subsequent tumor radical therapeutics. Mn^{2+} was released by the reaction of MnO_2 and intracellular GSH, which acted as the Fenton reaction catalyst to convert tumor-overexpressed H_2O_2 into ROS with the assistance of physiological HCO_3^-. (b) TEM image of MS@MnO_2 nanocatalysts. (c) Tumor-volume changes after varied treatments.[117] Copyright 2018, John Wiley and Sons. (d) Schematic illustration of the fabrication of mCMSNs and their therapeutic procedure for synergistic PDT and Fenton reaction-based synergistic tumor therapy.[118] Copyright 2019, American Chemical Society.

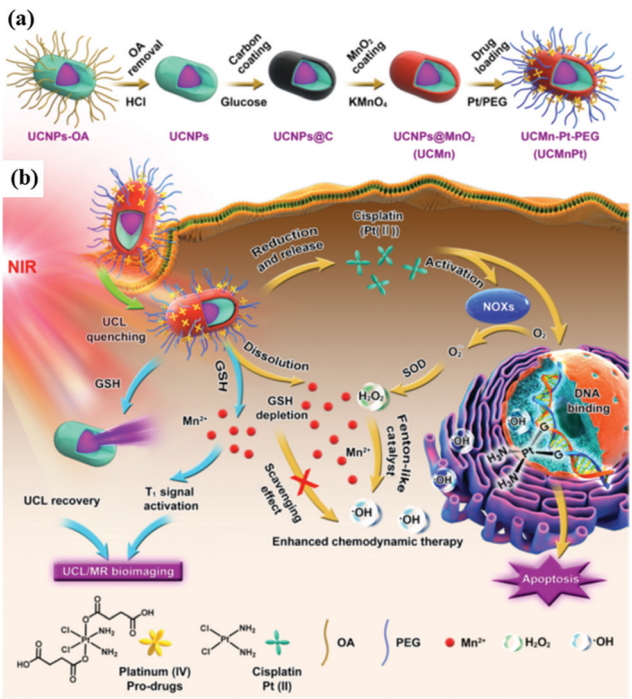

Fig. 8 Scheme illustrating the fabrication procedure for UCMnPt and their unique functionality for diagnostic imaging-guided synergistic chemotherapy and nanocatalytic tumor radical therapy.[119] Copyright 2019, American Chemical Society.

the paramagnetic nature of the Mn-based catalytic center is highly promising for T_1-weighted contrast-enhanced MR imaging, which provides the potential for therapeutic guidance and monitoring during this specific nanocatalytic radical therapy.

4. Carbon-based Fenton nanocatalysts

It has been well-demonstrated that carbon-based nanoplatforms exert high therapeutic potential in different diseases such as cancer,[120–122] bacterial infection[123–126] and brain-related diseases.[127–129] These carbon-based nanosystems typically include zero-dimensional carbon nanodots, one-dimensional carbon nanotubes and two-dimensional graphene oxides. Based on the background that carbon-involved materials have been extensively explored in catalytic chemistry and related catalytic applications, it is therefore reasonably expected that the rational design of the composition, nanostructure and physicochemical properties of carbon-based nanocatalysts could find biomedical applications such as Fenton-like reactions for nanotherapeutics. These metal-free carbon-based nanocatalysts also possess high biocompatibility due to the lack of toxicity on introducing metal ions into the body as compared with the most explored metal-based Fenton nanocatalysts.

Most Fenton nanocatalysts are based on metal-based nanoplatforms. Alternatively, some metal-free nanocatalysts such as carbon-based nanosystems have been extensively explored as electrocatalysts for versatile applications in energy storage,

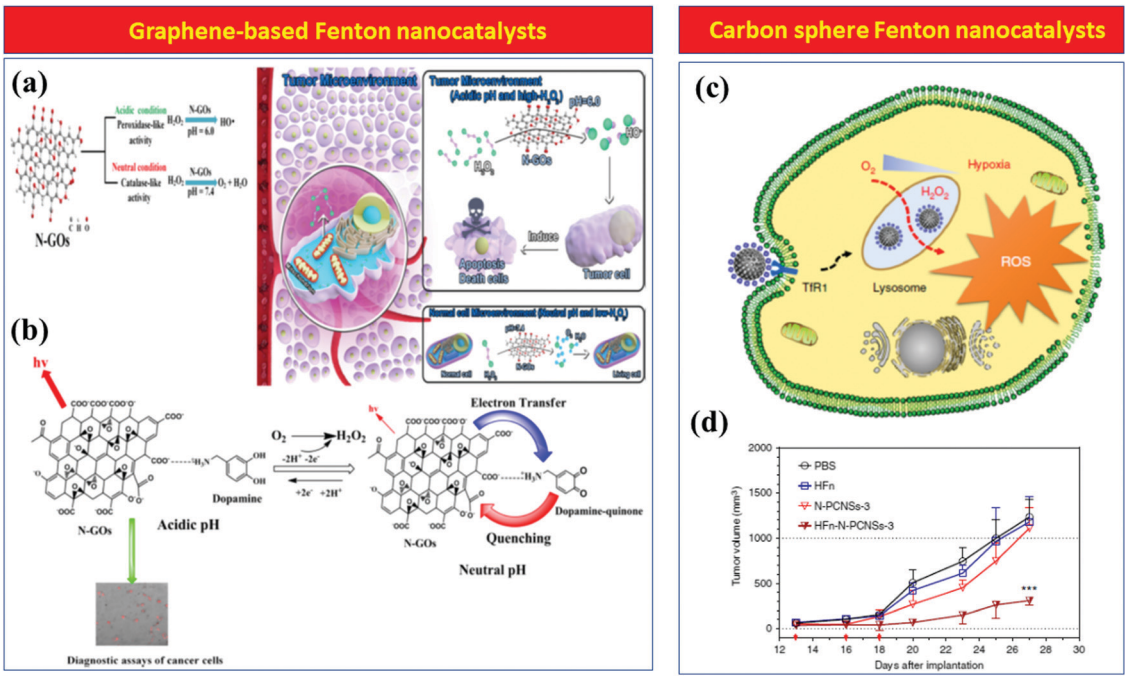

Fig. 9 (a) Schematic illustration of the intrinsic catalytic mechanism of N-GOs with different catalytic behaviors in tumor and normal-cell microenvironments. (b) The scheme of N-GOs with dopamine for turn-on fluorescence imaging of cancer cells while fluorescence quenching in normal cells.[130] Copyright 2019, American Chemical Society. (c) Schematic representation of N-PCNSs entering a tumor cell by ferritin-mediated specific endocytosis and inducing tumor-cell death by triggering an intracellular Fenton reaction *via* converting H_2O_2 into highly toxic hydroxyl radicals. (d) Tumor-volume changes after varied treatments, including targeted HFn-N-PCNSs-3 and non-targeted N-PCNSs-3.[131] Copyright 2018, Springer Nature.

photocatalysis, environment protection, *etc.* Their biomedical applications focus on drug delivery, photonic therapy, molecular imaging, and even tissue engineering. A recent breakthrough of carbon-based nanosystems is their unique catalytic properties in biomedicine, *i.e.*, they have been developed for nanocatalytic therapy by *in situ* triggering the Fenton reaction or exerting enzyme-mimicking performance. Graphene oxide nanoparticles (N-GOs) exhibited two different catalytic behaviors in tumor and normal cell microenvironments. The unique tumor-overexpressed H_2O_2 and mild acidity of the tumor microenvironment enabled N-GOs to act as Fenton nanocatalysts with peroxidase-like activity to generate hydroxyl ($^{\bullet}OH$) radicals (Fig. 9a), which were used to kill cancer cells and inhibit tumor growth.[130] Comparatively, N-GOs showed catalase-mimicking properties to convert H_2O_2 into O_2 under the neutral normal cell microenvironment, exhibiting no damage to normal cells. The integration of fluorescent N-GOs with dopamine made the selective fluorescence imaging of tumor cells possible based on the redox characteristics of dopamine (Fig. 9b). The oxidation of dopamine to produce dopamine-quinine quenched the N-GOs fluorescence in neutral conditions, but this effect did not occur in the acidic tumor microenvironment.

N-Doped carbon nanospheres (N-PCNSs) exhibited similar catalytic properties to graphene oxide.[131] These nanoparticles demonstrated four enzyme-mimicking properties, including oxidase, peroxidase, catalase and superoxide dismutase, where different conditions caused varied enzymatic activities. The nitrogen doping was important for enabling the catalytic performance of carbon nanospheres, and the higher nitrogen-doping amount induced higher catalytic activities (*e.g.*, N-PCNSs-3 indicating high N amount for performance evaluation). Ferritin was further used for the targeted delivery of N-PCNSs nanocatalysts into cell lysosome (designated as HFn-N-PCNSs-3). As a necessary condition for the Fenton-like reaction, the intracellular mild acidity activated HFn-N-PCNSs-3 for converting H_2O_2 into highly toxic hydroxyl ($^{\bullet}OH$) radicals (peroxidase activity, Fig. 9c), and the surface ferritin conjugation resulted in a tumor-specific catalytic Fenton reaction, achieving significant tumor regression in tumor-bearing mice (Fig. 9d).[131] It is noted that the peroxidase-mimicking activities of carbon materials, such as reduced graphene oxide or mesoporous carbon, could be significantly enhanced by hetero-atom nitrogen doping,[132] which was employed to develop high-performance biosensors for detecting bioactive molecules.[133] Such a radical nanotherapeutic modality was further explored in antibacterial and anti-biofilm applications, as it assisted with the supplementary photothermal conversion of carbonaceous frameworks for producing heat.[134,135]

5. Precious metal-based nanocatalysts (Ag, Ru and Pt)

Several types of precious metal-based nanosystems have found versatile applications in biomedicine. The most famous members of the precious metal nanofamily are silver (Ag) and gold (Au) nanoparticles, which have respectively exploded in

antibacterial[136–140] and NIR-triggered photothermal cancer therapy.[141–145] Other precious metals such as Pd,[146,147] Pt[148] and Ru[149,150] nanoparticles have also been demonstrated to be biocompatible and efficient in disease theranostics. It is noted that precious metals typically have high catalytic activities in abundant chemical reactions, which endow them with high potential in the catalytic Fenton-like chemical reaction for radical nanotherapeutics under the specific reaction conditions.

The Ag nanoparticles-mediated Fenton-like reaction has been demonstrated to be effective in inducing cancer-cell death or detecting biomolecule activity with oxidase-mimicking properties.[151,154] For instance, a Ag nanoparticle-based catalytic platform was constructed by TAMRA-DNA-templated synthesis of Ag nanoparticles onto the surface of graphene oxide nanosheets (designated as AgNPs–TAMRA-DNA@GO).[151] After endocytosis into cancer cells, the Ag component in AgNPs–TAMRA-DNA@GO catalyzed a Fenton-like reaction to generate $^{\bullet}OH$ and elevated the intracellular oxidative stress (Fig. 10a). In addition, Ag^{+} was concurrently released to induce cytotoxicity, which synergistically enhanced ROS-induced cytotoxicity. These AgNPs–TAMRA-DNA@GO nanocatalysts exhibited high cytotoxicity to cancer cells (HeLa cells) rather than normal cells (L02 cells) because tumor cell-overexpressed H_2O_2 could act as the reactant in the Fenton reaction as triggered by a catalytic procedure to generate cytotoxic $^{\bullet}OH$ and Ag^{+}.[151]

Hyaluronic acid-hybridized Ru nanoaggregates (designated as HA–Ru NAs) were constructed to achieve triple-modality nanotherapeutics, including Fenton reaction-based nanocatalytic therapy, PTT and PDT (Fig. 10b).[152] These HA–Ru NAs initially reacted with H_2O_2 under acidic conditions to produce Ru^{3+}, which would further convert H_2O_2 into hydroxyl ($^{\bullet}OH$) radicals, also under the acidic environment, inducing the intracellular oxidative stress for killing cancer cells. These HA–Ru NAs exhibited high photothermal-converting performance and photodynamic behavior as photothermal nanoagents and photosensitizers for PTT and PDT, respectively. The surface-conjugated hyaluronic acid enabled the targeted transportation of HA–Ru NAs into CD44-overexpressing cancer cells, achieving high *in vivo* tumor-suppressing efficacy. The specific nanoenzyme properties of Pt nanoparticles were investigated by constructing PtAu@SiO_2 nanoenzymes for reversing the multidrug resistance of cancer cells (Fig. 10c).[153] The Au component on the PtAu@SiO_2 nanoparticles was used to avoid the aggregation of neighboring ultrasmall Pt nanoparticles, while the SiO_2 core was used to hinder the quick clearance of small-sized PtAu. The intracellular acidic microenvironment triggered the corrosion of the Pt shell and subsequently induced the cytotoxic Pt ion release. These PtAu@SiO_2 not only acted as the catalase-like nanoenzyme to convert H_2O_2 into O_2 for alleviating tumor hypoxia but also induced ROS generation, such as highly toxic hydroxyl ($^{\bullet}OH$) radicals. The synergy of

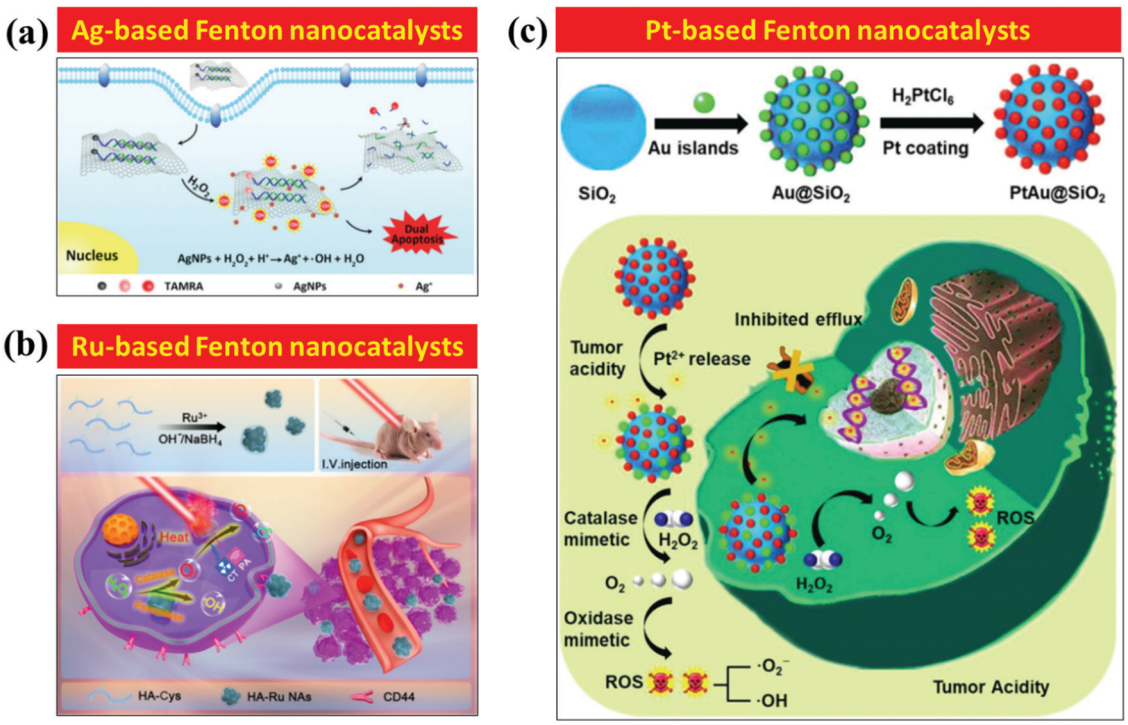

Fig. 10 (a) Schematic illustration of the intracellular behavior of AgNPs–TAMRA-DNA@GO nanocatalysts for triggering the Fenton reaction to produce $^{\bullet}OH$ and release Ag^{+}, inducing synergistic cancer-cell death.[151] Copyright 2018, Royal Society of Chemistry. (b) Schematic representation of the fabrication of HA–Ru NAs and their specific triple-modality nanotherapeutics such as Fenton reaction-based nanocatalytic therapy, PTT and PDT.[152] Copyright 2019, American Chemical Society. (c) Schematic illustration of the fabrication procedure of PtAu@SiO_2 nanoparticles and enzyme-mimicking nanoenzymes for exerting multiple biological performances in overcoming the drug resistance of cancer cells and inducing cancer cell death by ROS generation.[153] Copyright 2019, Royal Society of Chemistry.

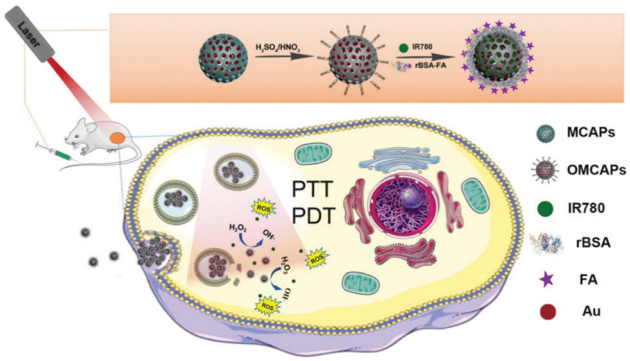

Fig. 11 The scheme of the fabrication process for OMCAPs@rBSA-FA@IR780 nanocomposites and their corresponding multifunctionalities for synergistic PTT, PDT and Au-catalyzed Fenton reaction-based nanocatalytic tumor radical therapy.[156] Copyright 2019, Ivyspring International Publisher.

released toxic Pt ions and generated ROS effectively reversed the multidrug resistance of cancer cells and induced cancer cell death.[153] MnO_2@PtCo nanoflowers were fabricated with both catalase and peroxidase-mimicking activity in the presence of H_2O_2 under acidic conditions (Fenton-like reaction), where the MnO_2 component decomposed H_2O_2 into oxygen to alleviate tumor hypoxia and the PtCo component converted H_2O_2 into hydroxyl radicals for inducing cancer-cell oxidative damage.[155]

In addition to the aforementioned precious metals such as Ag, Ru and Pt with catalytic performance for the Fenton reaction, gold (Au) nanoparticles have also been demonstrated to possess peroxidase-mimicking activity to trigger the Fenton reaction and subsequently convert H_2O_2 into •OH. Au nanoparticles were integrated into mesoporous carbon nanoparticles (designated as MCAPs), followed by the surface oxidation, NIR dye IR-780 loading and targeting molecule rBSA-FA surface conjugation (designated as OMCAPs@rBSA-FA@IR780, Fig. 11).[156] This OMCAPs@rBSA-FA@IR780 exhibited synergistic therapeutic efficacy originating from each functionality of every component. The integrated Au nanoparticles acted as the nanocatalysts to trigger the Fenton-like reaction and produced hydroxyl radicals for oxidative tumor therapy. The mesoporous carbon matrix converted photonic energy into thermal energy for tumor ablation, and the loaded IR780 acted as the photosensitizer for PDT.

6. Other iron-free nanocatalysts for therapeutic biomedicine

In addition to the aforementioned Cu, Mn, precious-metal-based and carbon-based Fenton nanocatalysts in biomedicine, the intrinsic catalytic properties of versatile metal-based nanoplatforms enabled the emergence of other versatile Fenton nanocatalysts, including W, Co, Ce and Bi-based nanosystems. These nanocatalysts not only can trigger the Fenton reaction for radical nanotherapeutics, but also possess additional properties for augmenting the catalytic-therapeutic efficacy and synergistically enhancing the total therapeutic outcome.

WO_{3-x} nanoparticles have been developed as the photothermal nanoagents for photonic tumor ablation.[159–161] There exist both W^{5+} and W^{6+} species in WO_{3-x}, indicating the high potential of WO_{3-x} as Fenton nanocatalysts for nanocatalytic tumor therapy. As a paradigm, WO_{3-x}@γ-PGA (γ-PGA: γ-poly-L-glutamic acid) nanocatalysts were fabricated, employing γ-PGA as the ligand to modulate the size and topology of the WO_{3-x} nanoparticles (Fig. 12a and b).[157] The Fenton-like reaction was triggered by WO_{3-x}@γ-PGA as nanocatalysts to convert H_2O_2 into hydroxyl radicals (•H_2O) based on the presence of W^{5+}/W^{6+} pairs. Importantly, this WO_{3-x}@γ-PGA-catalyzed Fenton reaction to produce oxidative stress was further enhanced by the NIR-triggered photothermal effect, which could elevate the local temperature to accelerate the Fenton reaction rate, and was demonstrated by the larger production of •OH and enhanced tumor-suppression efficacy (Fig. 12c). Chemotherapeutic doxorubicin (DOX)-loaded cobalt oxide nanoprisms (Co_3O_4–DOX) were fabricated for degradation-induced nanocatalytic therapy based on the Fenton reaction.[158] The unique tumor microenvironment of overexpressed H_2O_2 and mild acidity enabled the degradation of Co_3O_4 nanoprisms to release Co^{3+}, which not only resulted in the T_2-to-T_1 switching of the MR imaging contrast, but also acted as the catalysts to trigger the Fenton reaction for converting H_2O_2 into hydroxyl (•OH) radicals and subsequently inducing cancer-cell death (Fig. 12d). The synergy of the chemotherapy (DOX), photothermal ablation and Fenton reaction-based nanocatalytic effect significantly suppressed the tumor growth.

Metal–organic frameworks (MOFs) with versatile compositions have been demonstrated to exert the nanocatalyst functionality for triggering the Fenton reaction and the subsequent nanotherapeutics. The underlying mechanism is the catalytic conversion of H_2O_2 into hydroxyl (•OH) radicals. The Au-doped MOF NIL-88B (MOF–Au) integrated with Ce nitrilotriacetic acid (NTA) complexes (MOF–Au–Ce) was constructed to exert two specific functionalities for antibacterial and anti-biofilm performance (Fig. 13a).[162] On the one hand, the Au doping enhanced the catalytic activity of the MOF based on the synergistic effect between Au and MOF, resulting in the efficient production of •OH for killing bacterial cells. On the other hand, the integrated Ce^{IV} targeted and hydrolyzed extracellular DNA (eDNA) for biofilm disintegration and bacterial death. Such a synergistic performance substantially eradicated biofilms, as demonstrated by the admirable bactericidal effects *in vivo* against subcutaneous abscess on mice after the treatments with MOF–Au–Ce and H_2O_2 (Fig. 13b).

Cerium (Ce) has different valences such as Ce^{4+} and Ce^{3+} in the form of oxides. The reversible conversion between Ce^{4+} and Ce^{3+} could trigger a series of catalytic reactions. For instance, a similar Fenton-like reaction was triggered by employing a core/shell nanoparticle with mesoporous cerium oxide as the shell and upconversion nanoparticles (UCNPs) as the core (designated as UCNPs@mCeO_x).[163] Initially, the mCeO_x component triggered endogenous H_2O_2 decomposition to generate O_2.

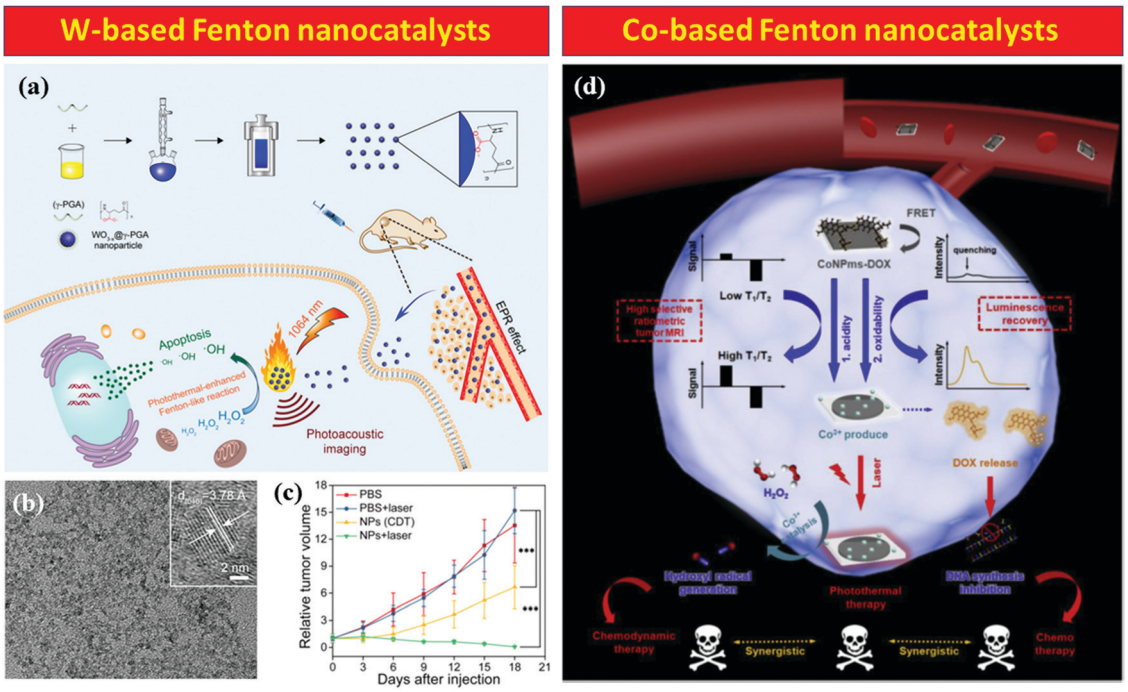

Fig. 12 (a) Schematic illustration of the construction of WO_{3-x}@γ-PGA nanoagents for synergistic PTT and photothermal-enhanced Fenton reaction-based nanocatalytic tumor therapy. (b) TEM image of WO_{3-x}@γ-PGA nanoparticles. (c) Tumor-volume change after varied treatments.[157] Copyright 2018, American Chemical Society. (d) Scheme showing a DOX-loaded Co_3O_4 nanoprism for redox/pH-responsive degradation in cancer cells, enabling T_1/T_2 ratiometric MR imaging-guided synergistic cancer therapy based on photothermal ablation and Fenton reaction-based nanocatalytic therapy.[158] Copyright 2018, Elsevier.

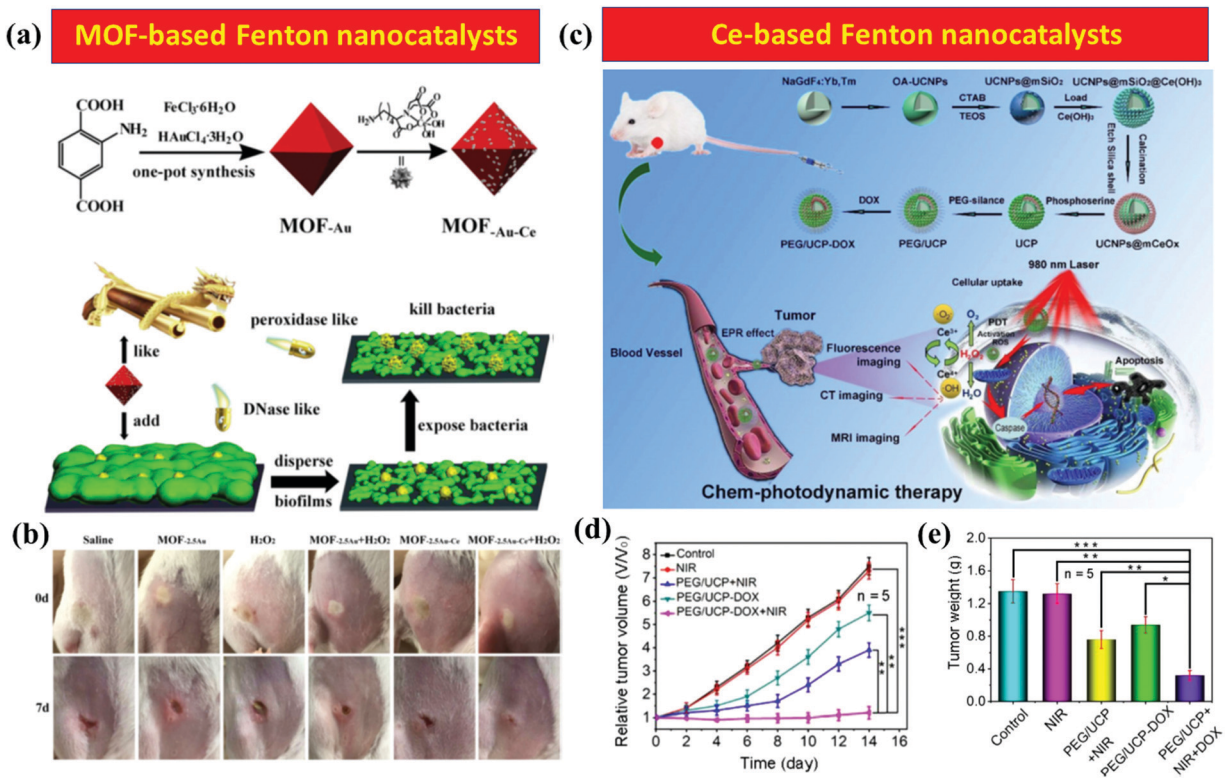

Fig. 13 (a) Scheme showing the construction of MOF–Au–Ce with antibacterial and anti-biofilm performance and the underlying related mechanism. (b) Photographic images of subcutaneous abscesses on mice in different treatment groups.[162] Copyright 2019, Elsevier. (c) Schematic illustration of the construction of PEG/UCNP-DOX nanoplatforms and their multiple therapeutic functionalities. (d) Tumor-volume and (e) tumor-weight changes after varied treatments.[163] Copyright 2019, Royal Society of Chemistry.

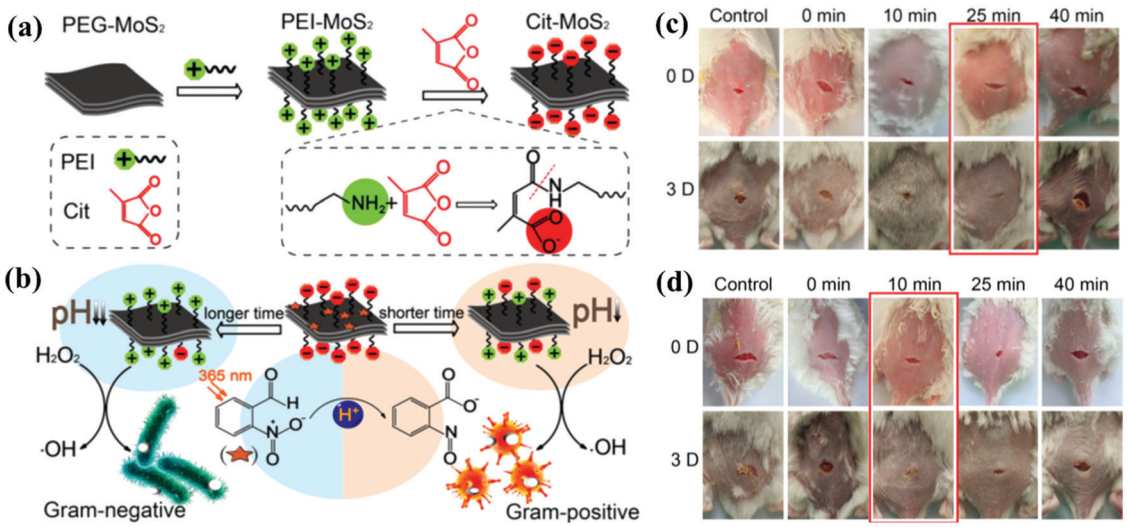

Fig. 14 (a) Schematic representation of the construction of Cit-MoS_2(III). (b) Gram-selective antimicrobial activity by light-modulated Cit-MoS_2(III) nanoenzymes. (c) Photographic images of wound sites on mice after infection with (c) *E. coli* and (d) *S. aureus*, followed by varied treatments among different groups with varied light irradiation durations at the wavelength of 365 nm (control: PBS buffer; treatment group: 2-NBA + Cit-MoS_2(III) + H_2O_2 with varied light-irradiation durations).[165] Copyright 2018, American Chemical Society.

Then, the UCNPs core converted NIR into UV light, which further activated the $mCeO_2$ shell to produce electron–hole pairs, and subsequently converted the generated O_2 into superoxide radicals ($^{\bullet}O_2^-$) and H_2O_2/H_2O into hydroxyl ($^{\bullet}OH$) radicals (Fig. 13c). The combination of such a NIR-triggered catalytic procedure for ROS production and DOX-based chemotherapy achieved desirable tumor-suppression efficacy against murine cervical carcinoma in mice (Fig. 13d and e).[163] In addition, the CeO_2 nanoparticles-dispersed porous carbonaceous framework was constructed from nanoscale cerium-based MOFs for synergistic cancer therapy based on their intrinsic oxidase-mimicking property-induced oxidative therapy, reduced energy-supply performance and desirable drug-delivery capacity.[164]

MoS_2 nanosheets exhibited catalytic capability in the Fenton reaction, and have been used as antibacterial agents to prevent infection. To achieve Gram-selective antimicrobial properties, MoS_2 nanosheets were surface modified stepwise with polyethylene glycol (PEG–MoS_2(I)), polyethyleneimine (PEI–MoS_2(II)) and citraconic anhydride-modified PEI–MoS_2(II) (Cit-MoS_2(III), Fig. 14a).[165] These Cit-MoS_2(III) achieved intelligent light-triggered charge conversion with the assistance of a photoacid generator, 2-nitrobenzaldehyde (2-NBA). By controlling the photonic irradiation duration, the pH of the microenvironment was reduced, which induced different proportions of surface positive charge for Cit-MoS_2(III). The pH-lowing effect also enhanced the catalytic activation of Cit-MoS_2(III) on converting

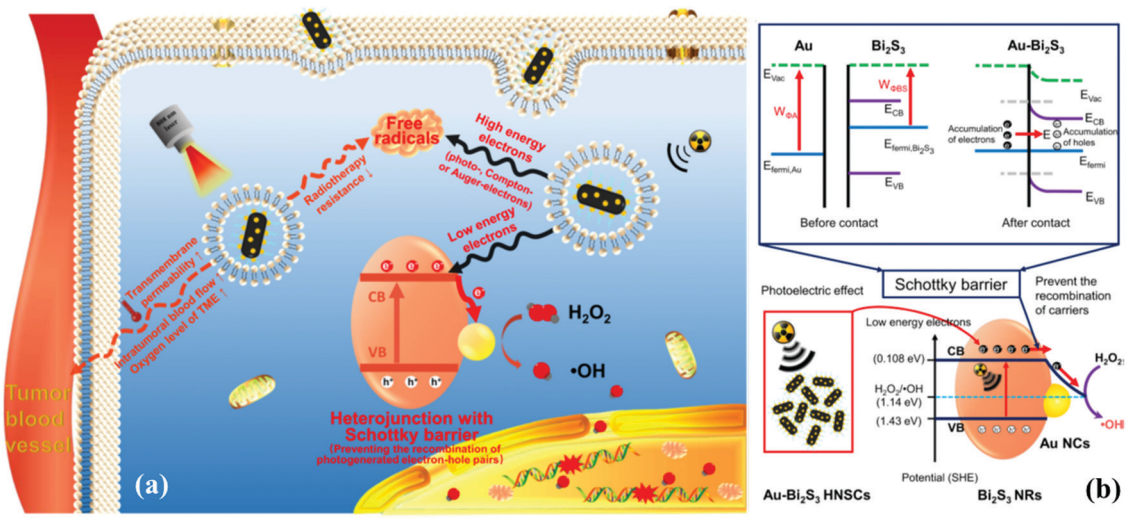

Fig. 15 (a) Schematic representation of the unique therapeutic functionality of heterogenous Au–Bi_2S_3 nanocomposites for the X-ray-activated catalytic process to convert H_2O_2 into hydroxyl radicals. (b) The intrinsic mechanism for the X-ray-activated catalytic process to produce hydroxyl radicals by the Schottky-type Au–Bi_2S_3 heterostructure.[166] Copyright 2019, American Chemical Society.

H_2O_2 into hydroxyl radicals for antibacterial activity (Fig. 14b). Therefore, the photo-modulated surface positive charge and catalytic activity of Cit-MoS_2(III) enabled the Gram-selective antimicrobial outcome. The *in vivo* results (Fig. 14c and d) demonstrated that the treatment of bacteria-infected mice with Cit-MoS_2(III) and 2-NBA followed by 10 min of light irradiation (λ = 365 nm) achieved effective therapy for *S. aureus* infection. Comparatively, the longer light irradiation duration of 25 min induced effective therapy for *E. coli* infection with no side effects to major organs. The different antibacterial properties of Cit-MoS_2(III) after varied light irradiation provided solid evidence of the Gram-selective antibacterial performance.

The nanocatalyst-activated Fenton-like reaction can also be triggered/enhanced by exogenous X-ray irradiation. As a typical paradigm, Au–Bi_2S_3 metal–semiconductor hetero-nanostructure composites were constructed with Schottky barriers for X-ray-activated H_2O_2 conversion into hydroxyl ($^{\bullet}OH$) radicals.[166] Based on the high-*Z* Bi and Au elements in Au–Bi_2S_3, the high radiation dose was deposited in tumors to generate high-energy electrons. In addition, the X-ray activation also triggered the generation of low-energy electron–hole pairs, and the presence of the Schottky barrier of Au–Bi_2S_3 enabled the quick and efficient separation and transfer of these electrons and holes to the surface of Au and Bi_2S_3, inducing the enhanced generation efficacy of electron–hole pairs. The X-ray-generated electron–hole pairs were capable of inducing tumor-overexpressed H_2O_2 into $^{\bullet}OH$ by a catalytic procedure, which was oxygen-independent and thus beneficial for hypoxic tumor treatment (Fig. 15a). The presence of the Schottky barrier was favorable for trapping the X-ray activation-generated electrons and transferring them to the Au components, enabling efficient separation and preventing the recombination of the generated electron–hole pairs for decomposing H_2O_2 into $^{\bullet}OH$ radicals (Fig. 15b).[166]

7. Conclusions and outlook

Catalytic nanomedicine has become one of the most important research frontiers in theranostic biomedicine, in which the nanocatalytic Fenton reaction represents the most explored therapeutic modality based on the conversion of intrinsic disease-overexpressed or exogenously introduced H_2O_2 into highly toxic hydroxyl ($^{\bullet}OH$) radicals under specific acidic conditions. Based on the disease-specific features, this Fenton reaction-based nanocatalytic therapy possesses high therapeutic efficacy and biosafety, *i.e.*, it can selectively attack tumors but causes no harm/damage to normal cells/tissues. Most Fenton nanocatalysts are based on Fe-based nanoparticles, but they suffer from the necessary requirements of strong acidity and low catalytic rate, causing low therapeutic efficacy. As such, alternative iron-free nanocatalysts are currently undergoing extensive research. Versatile iron-free nanocatalysts have been developed as nanocatalysts for trigging the Fenton reaction in order to achieve different therapeutic purposes, including Cu-based, Mn-based, W-based, Co-based, Ce-based, Mo-based, precious metals (*e.g.*, Ag, Ru, Pt, Au), and even nonmetals such as carbon-based nanosystems (Table 1). Most of these iron-free Fenton nanocatalysts have intrinsic catalytic characteristics for disease therapeutics, such as easy operation in a wide pH range, high reaction rate, exogenous-responsive Fenton-reaction behavior, photothermal/photodynamic-enhanced catalytic efficacy, *etc.* Most of these iron-free nanocatalysts are used for cancer therapy, in addition to some antibacterial and antibiofilm applications. The reaction conditions for these iron-free nanocatalysts in Fenton-based reaction can be controlled to enhance the therapeutic efficacy, which involves the local temperature, acidity, hydrogen peroxide amount, and external activation such as ultrasound irradiation. The precise modulation of these reaction conditions can control the reaction rate and efficiency; *e.g.*, elevating the local temperature, enhancing the acidity, increasing the hydrogen peroxide amount and external ultrasound irradiation.

Although these iron-free nanocatalysts are highly promising for Fenton reaction-based nanocatalytic therapy, it should be noted that the research in this research frontier is still in its infancy. The current research mainly focuses on the development of new intriguing iron-free Fenton nanocatalysts and their preliminary catalytic performance evaluation in nanotherapeutics, leaving many unresolved issues hindering further broad biomedical applications and potential future clinical translations, as mainly discussed below and in Fig. 16.

It has been well demonstrated that the biocompatibility and biosafety of iron-based nanoparticles have been extensively evaluated, and there is solid evidence in support of their desirable and intriguing biosafety to guarantee their potential further clinical translation. However, most iron-free nanocatalysts are based on metal-based nanocatalysts, but the biocompatibility and biosafety of these iron-free nanocatalysts have not been thoroughly investigated. From the viewpoint of composition, the potential cytotoxicity of some iron-free nanocatalysts such as Cu, Mn, Co, Mo and Ce is higher than that of Fe. Though nanoparticulate formulation of these iron-free nanocatalysts mitigates their toxicity, the specific biological effect and biosafety still require strict evaluation. Metal-free nanocatalysts such as carbon nanoparticles suffer from low-biodegradability issues, which is still an unresolved problem for most inorganic iron-free Fenton nanocatalysts. Mn-Based nanocatalysts exhibit specific tumor-sensitive disintegration and biodegradation, which might be beneficial for their easy excretion from the body. Based on the above consideration, the following studies should take full consideration of this critical issue regarding the biological effects, biocompatibility, biodegradability and biosafety, which play determining roles in their potential clinical translation.

The emerging nanocatalytic medicines are still in the preliminary stages for versatile biomedical applications. Therefore, the underlying catalytic mechanism is still unclear to some extent. Although the Fenton reaction has been extensively explored in catalytic chemistry and the related catalytic procedure and mechanism have been thoroughly revealed, the iron-free nanocatalysts-triggered Fenton reaction in diseased cells and

Table 1 Selected paradigms of iron-free Fenton nanocatalysts for biomedical applications

Num.	Basic element	Iron-free Fenton nanocatalysts	Therapeutic modality	Theranostic performance and outcome	Ref.
1	Cu	Cu–cysteine mercaptide	Fenton radical therapy	Consuming GSH for enhancing Fenton therapeutic efficacy with much higher therapeutic outcome as compared to DOX	71
2	Cu	Copper peroxide nanodots	Fenton radical therapy	H_2O_2-self-supplying Fenton reaction for suppressing the growth of tumor	72
3	Cu	Cu/SOD-loaded $CaCO_3$	Fenton radical therapy	Sequential reaction with H_2O_2-self-supplying and specific toxicity to cancer cells	73
4	Cu	$Cu_2(OH)PO_4$	Fenton radical therapy	X-ray irradiation to convert Cu^{II} sites into Cu^{I} sites and subsequent radical therapy on tumor therapy	75
5	Cu	$Cu_{2-x}S$	Fenton radical therapy and PTT	PTT-synergistic and PTT-enhanced Fenton radical therapy for inhibiting the tumor growth	76
6	Cu	Cu_2Se	Fenton radical therapy and PTT	NIR-II-activated photothermal-enhanced nanocatalytic efficacy of Fenton reaction on tumor therapy	77
7	Cu	C-m-ABs	Fenton radical therapy, PDT and PTT	Light-enhanced radical therapy with the synergy of PDT and PTT on tumor therapy	78
8	Cu	Cu-HMSNs	Fenton radical therapy and chemotherapy	Cu^{2+} ions-activated DSF chemotherapy and Cu^{+} ions-catalyzed Fenton radical therapy on tumor therapy	85
9	Cu	$Cu(DDC)_2$	Fenton radical therapy and chemotherapy	$Cu(DDC)_2$-induced chemotherapy and the residual Cu(II)-initialized Fenton reaction-induced radical ($^{\bullet}OH$) oxidative therapy	86
10	Cu	Cu^{2+}-g-C_3N_4	Fenton radical therapy and PDT	Depletion of intracellular GSH level for Cu^{2+}-catalyzed Fenton-like reaction and photo-activated photodynamic ROS generation	95
11	Cu	Cu-MOF	Fenton radical therapy, PDT and immunotherapy	Synergistic inhibition of primary tumors and efficient suppression of distant tumors	96
12	Cu	Cu-DMONs	Fenton radical therapy, chemotherapy and immunotherapy	Enhanced and synergistic chemo-immunotherapeutic efficacy for inhibiting primary and distant tumors	97
13	Mn	MS@MnO_2	Fenton radical therapy	Deplete intracellular GSH to avoid $^{\bullet}OH$ consumption and enhance radical therapy on combating tumor	117
14	Cu, Mn	CMSNs	Fenton radical therapy and PDT	GSH depletion for augmenting the radical-based therapeutic efficacy	118
15	Mn	MnO_2–UCNP	Fenton radical therapy and chemotherapy	GSH depletion and H_2O_2-self-supplying for enhanced radical therapy and synergistic chemotherapy on tumor therapy	119
16	C	N-GOs	Fenton radical therapy	Peroxidase-like activity to generate hydroxyl ($^{\bullet}OH$) radicals for killing cancer cells and inhibiting tumor growth	130
17	C	N-PCNSs	Fenton radical therapy	Targeted tumor radical therapy with high specificity and therapeutic efficacy	131
18	Ag	Ag–GO	Fenton radical therapy	Generating $^{\bullet}OH$ and elevating the intracellular oxidative stress with the synergy of Ag^{+} cytotoxicity	151
19	Ru	HA–Ru	Fenton radical therapy, PDT and PTT	Targeted tumor therapy with combined Fenton radical therapy, PDT and PTT	150
20	Au	MCAPs	Fenton radical therapy, PDT and PTT	Synergistic Fenton radical tumor therapy, PDT and PTT	156
21	W	WO_{3-x}	Fenton radical therapy and PTT	NIR-triggered photothermal effect for enhancing Fenton radical tumor therapy	157
22	Co	Co_3O_4–DOX	Fenton radical therapy, PTT and chemotherapy	Enhanced Fenton radical tumor therapy with the synergy of PTT and chemotherapy	158
23	Ce	UCNPs@$mCeO_x$	Fenton radical therapy,	NIR-UV light conversion for enhancing Fenton radical tumor therapy	163
24	Mo	MoS_2 nanosheets	Fenton radical therapy	Photo-modulated Gram-selective antimicrobial property both *in vitro* and *in vivo*	165
25	Au, Bi	Au–Bi_2S_3	Fenton radical therapy	X-ray-generated electron–hole pairs for inducing tumor-overexpressed H_2O_2 into $^{\bullet}OH$ and therapy of hypoxic tumor	166

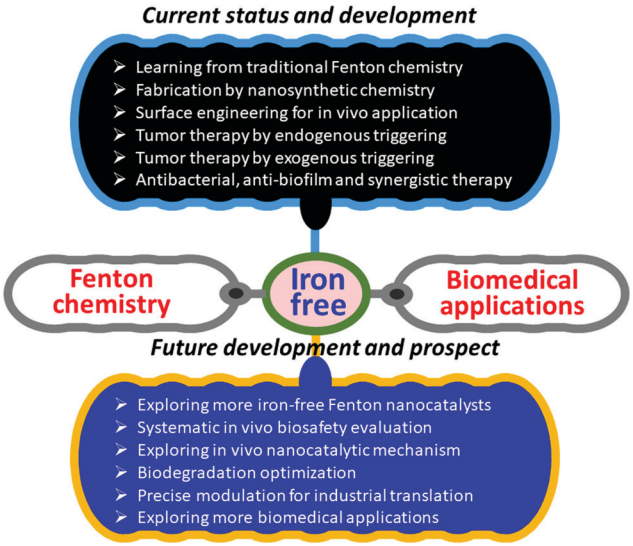

Fig. 16 Schematic representation of the current status/development and future development/prospects of iron-free Fenton nanocatalysts for versatile biomedical applications.

tissues is difficult to probe *in situ*. Because of the highly complex *in vitro* (intracellular level) and *in vivo* (animal model) microenvironments and conditions, most of the reaction procedure and mechanism originate from the speculation of the catalytic Fenton reaction in catalytic chemistry. There is still a lack of related techniques for revealing the reaction procedure *in situ*, especially for determining the intermediates during the Fenton reaction in cells or tissues. It should be noted that the knowledge regarding this reaction mechanism is highly important for further optimizing the catalytic properties of iron-free nanocatalysts. In addition, investigations on the catalytic procedure for iron-free nanocatalysts in the Fenton reaction are much less as compared to iron nanocatalysts, even in traditional catalytic chemistry, making it more difficult to determine the exact mechanism. Some exogenously triggered Fenton reactions by some iron-free nanocatalysts are based on traditional catalytic chemistry. It is still unclear whether such a catalytic process suits the biomedical process in cells or tissues. Therefore, subsequent research should focus on the underlying catalytic mechanisms by some advanced techniques or related instruments, providing the fundamentals for optimizing and enhancing the catalytic efficacy for satisfying the biomedical requirements.

The current development of nanomedicine and nanobiotechnology faces a great challenge of nanoparticle targeting of lesion sites, which is of critical significance for guaranteeing high therapeutic efficacy and low adverse effects on normal cells/tissues. These iron-free nanocatalysts also suffer from this critical issue. Although Fenton-based nanocatalysts only trigger the chemical reaction in diseased cells/tissues by producing highly toxic hydroxyl radicals and leaving normal cells/tissues undamaged, the non-specific accumulation of these nanocatalysts would not only lower the therapeutic efficacy but also cause potential long-term biosafety issues because of the high accumulation of these iron-free nanocatalysts. Most of the nanocatalysts are based on the enhanced permeability and retention (EPR) effect, but such a passive-targeting efficacy is rather low, typically less than 5%. Some surface-targeting conjugations with antibodies or targeting molecules somewhat enhance the accumulation efficacy, but this active targeting is still far from satisfactory. Fortunately, for this disease-specific Fenton reaction by biocompatible iron-free nanocatalysts, the accepted dose of these nanocatalysts is much higher as compared to traditional chemotherapeutic agents. It is still highly expected that adequate targeting strategies should be explored to enhance the nanocatalyst accumulation in lesion tissue/cells because it can at least improve the therapeutic efficacy.

The fabrication methodologies for these iron-free nanocatalysts are still not mature, which means that the precise modulation of the nanostructure, composition and corresponding catalytic properties is still highly difficult. Most of these iron-free nanocatalysts are newly emerging nanosystems, and therefore the related synthetic approaches are severely lacking as compared to the mostly explored Fe-based nanosystems. Because the current study on Fenton-based nanocatalytic medicine is still at the stage of conceptual demonstration, current research is focused on exploring the new iron-free nanocatalysts but much fewer efforts are devoted to detailed nanocatalyst modulation of nanostructure and composition, not to mention large-scale production, which is highly necessary for further industrial translation/production. It is still difficult to distinguish which iron-free nanocatalyst is more promising for further clinical translation at the current stage. Therefore, in the future exploration of new iron-free nanocatalysts special attention should be paid to the fabrication methodology, which is mainly based on the development of nanosynthetic chemistry.

Fenton reaction-based nanotherapeutics enabled by iron-free nanocatalysts have not found broad biomedical applications. Most of their uses are in tumor nanotherapeutics, with few reports on antibacterial or antibiofilm performance. Based on the high therapeutic efficacy and biosafety of this disease-specific modality, it is highly believed and expected that they would find more adequate biomedical applications in versatile biomedicine, which undoubtedly requires that more collaborations and efforts from researchers from different fields/backgrounds should be devoted to this fascinating research frontier.

As a new but highly promising research frontier of theranostic nanomedicine, Fenton reaction-based nanocatalytic biomedicines have shown disease-specific features with high therapeutic efficacy and biosafety with the assistance of these iron-free nanocatalysts. With the fast development of nanomedicine and advanced nanosynthetic chemistry, more iron-free nanocatalysts are expected to be developed for versatile biomedical use, and some of these nanocatalysts will enter clinical trials or even clinical stages provided that the aforementioned critical issues are adequately solved. Finally, it is concluded that these iron-free nanocatalysts-enabled Fenton reaction-based nanocatalytic therapeutics provide totally different therapeutic ideas with concurrently high efficacy and biosafety, as compared to traditional chemotherapy with severe side effects to normal cells/tissues.

Conflicts of interest

There are no conflicts to declare.

Acknowledgements

We greatly acknowledge the financial support from the National Key R&D Program of China (Grant No. 2016YFA0203700), National Natural Science Foundation of China (Grant No. 81760317, 81871365, 51672303), Excellent Young Scientist Foundation of NSFC (Grant No. 51722211), Key Projects of Hainan Province (Grant No. ZDYF2019136) and Program of Shanghai Subject Chief Scientist (Grant No. 18XD1404300).

References

1 T. Lammers, S. Aime, W. E. Hennink, G. Storm and F. Kiessling, *Acc. Chem. Res.*, 2011, **44**, 1029–1038.
2 B. Yang, Y. Chen and J. Shi, *Adv. Mater.*, 2019, DOI: 10.1002/adma.201901778.
3 K. Riehemann, S. W. Schneider, T. A. Luger, B. Godin, M. Ferrari and H. Fuchs, *Angew. Chem., Int. Ed.*, 2009, **48**, 872–897.
4 B. Yang, Y. Chen and J. Shi, *Chem. Rev.*, 2019, **119**, 4881–4985.
5 J. Shi, P. W. Kantoff, R. Wooster and O. C. Farokhzad, *Nat. Rev. Cancer*, 2017, **17**, 20–37.
6 H. Xiang and Y. Chen, *Small*, 2019, **15**, 1805339.
7 S. Pan, Y. S. Li and J. L. Shi, *J. Inorg. Mater.*, 2018, **33**, 1097–1102.
8 S. Y. Fu, B. Yu, H. F. Ding, G. D. Shi and Y. F. Zhu, *J. Inorg. Mater.*, 2019, **34**, 444–454.
9 S. Lal, S. E. Clare and N. J. Halas, *Acc. Chem. Res.*, 2008, **41**, 1842–1851.
10 W. Yin, L. Yan, J. Yu, G. Tian, L. Zhou, X. Zheng, X. Zhang, Y. Yong, J. Li, Z. Gu and Y. Zhao, *ACS Nano*, 2014, **8**, 6922–6933.
11 L. Cheng, J. Liu, X. Gu, H. Gong, X. Shi, T. Liu, C. Wang, X. Wang, G. Liu, H. Xing, W. Bu, B. Sun and Z. Liu, *Adv. Mater.*, 2014, **26**, 1886–1893.
12 X. Zhen, X. Feng, C. Xie, Y. Zheng and K. Pu, *Biomaterials*, 2017, **127**, 97–106.
13 L. E. Deng, Y. Li, L. Gong and J. Wang, *Acc. Chem. Res.*, 2018, **33**, 825–831.
14 Z. Liu, H. Lin, M. Zhao, C. Dai, S. Zhang, W. Peng and Y. Chen, *Theranostics*, 2018, **8**, 1648–1664.
15 P. Zhu, Y. Chen and J. Shi, *ACS Nano*, 2018, **12**, 3780–3795.
16 X. Qian, Y. Zheng and Y. Chen, *Adv. Mater.*, 2016, **28**, 8097–8129.
17 W. Yue, L. Chen, L. Yu, B. Zhou, H. Yin, W. Ren, C. Liu, L. Guo, Y. Zhang, L. Sun, K. Zhang, H. Xu and Y. Chen, *Nat. Commun.*, 2019, **10**, 2025.
18 Y. Cao, Y. Chen, T. Yu, Y. Guo, F. Liu, Y. Yao, P. Li, D. Wang, Z. Wang, Y. Chen and H. Ran, *Theranostics*, 2018, **8**, 1327–1339.
19 X. Liu, J. Zheng, W. Sun, X. Zhao, Y. Li, N. Gong, Y. Wang, X. Ma, T. Zhang, L.-Y. Zhao, Y. Hou, Z. Wu, Y. Du, H. Fan, J. Tian and X.-J. Liang, *ACS Nano*, 2019, **13**, 8811–8825.
20 C. Kumar and F. Mohammad, *Adv. Drug Delivery Rev.*, 2011, **63**, 789–808.
21 Y. Chen, L. Jiang, R. Wang, M. Lu, Q. Zhang, Y. Zhou, Z. Wang, G. Lu, P. Liang, H. Ran, H. Chen and Y. Zheng, *Adv. Mater.*, 2014, **26**, 7468–7473.
22 J. H. Lee, J. T. Jang, J. S. Choi, S. H. Moon, S. H. Noh, J. W. Kim, J. G. Kim, I. S. Kim, K. I. Park and J. Cheon, *Nat. Nanotechnol.*, 2011, **6**, 418–422.
23 G. Mikhaylov, U. Mikac, A. A. Magaeva, V. I. Itin, E. P. Naiden, I. Psakhye, L. Babes, T. Reinheckel, C. Peters and R. Zeiser, *Nat. Nanotechnol.*, 2011, **6**, 594–602.
24 S. Mura, J. Nicolas and P. Couvreur, *Nat. Mater.*, 2013, **12**, 991–1003.
25 Y. Geng, P. Dalhaimer, S. S. Cai, R. Tsai, M. Tewari, T. Minko and D. E. Discher, *Nat. Nanotechnol.*, 2007, **2**, 249–255.
26 J. J. Song, B. Chen and K. L. Lin, *J. Inorg. Mater.*, 2018, **33**, 623–628.
27 X. Han, X. Jing, D. Yang, H. Lin, Z. Wang, H. Ran, P. Li and Y. Chen, *Theranostics*, 2018, **8**, 4491–4508.
28 D. Putnam, *Nat. Mater.*, 2006, **5**, 439–451.
29 F. Torney, B. G. Trewyn, V. S. Y. Lin and K. Wang, *Nat. Nanotechnol.*, 2007, **2**, 295–300.
30 D. W. Pack, A. S. Hoffman, S. Pun and P. S. Stayton, *Nat. Rev. Drug Discovery*, 2005, **4**, 581–593.
31 H.-W. Yang, M.-Y. Hua, T.-L. Hwang, K.-J. Lin, C.-Y. Huang, R.-Y. Tsai, C.-C. M. Ma, P.-H. Hsu, S.-P. Wey, P.-W. Hsu, P.-Y. Chen, Y.-C. Huang, Y.-J. Lu, T.-C. Yen, L.-Y. Feng, C.-W. Lin, H.-L. Liu and K.-C. Wei, *Adv. Mater.*, 2013, **25**, 3605–3611.
32 R. Liang, Y. Chen, M. Huo, J. Zhang and Y. Li, *Nanoscale Horiz.*, 2019, **4**, 890–901.
33 Y. You, Z. Wang, H. Ran, Y. Zheng, D. Wang, J. Xu, Z. Wang, Y. Chen and P. Li, *Nanoscale*, 2016, **8**, 4324–4339.
34 M. Huo, L. Wang, Y. Wang, Y. Chen and J. Shi, *ACS Nano*, 2019, **13**, 2643–2653.
35 M. Huo, L. Wang, Y. Chen and J. Shi, *Nat. Commun.*, 2017, **8**, 357.
36 S. Kwon, H. Ko, D. G. You, K. Kataoka and J. H. Park, *Acc. Chem. Res.*, 2019, **52**, 1771–1782.
37 X. Qian, J. Zhang, Z. Gu and Y. Chen, *Biomaterials*, 2019, **211**, 1–13.
38 Z. Dong, L. Feng, Y. Chao, Y. Hao, M. Chen, F. Gong, X. Han, R. Zhang, L. Cheng and Z. Liu, *Nano Lett.*, 2019, **19**, 805–815.
39 J.-X. Fan, M.-Y. Peng, H. Wang, H.-R. Zheng, Z.-L. Liu, C.-X. Li, X.-N. Wang, X.-H. Liu, S.-X. Cheng and X.-Z. Zhang, *Adv. Mater.*, 2019, **31**, 1808278.
40 C. Walling, *Acc. Chem. Res.*, 1998, **31**, 155–157.
41 E. Neyens and J. Baeyens, *J. Hazard. Mater.*, 2003, **98**, 33–50.
42 M. Cheng, C. Lai, Y. Liu, G. M. Zeng, D. L. Huang, C. Zhang, L. Qin, L. Hu, C. Y. Zhou and W. P. Xiong, *Coord. Chem. Rev.*, 2018, **368**, 80–92.

43 Z. M. Tang, Y. Y. Liu, M. Y. He and W. B. Bu, *Angew. Chem., Int. Ed.*, 2019, **58**, 946–956.
44 Y. P. Zhu, R. L. Zhu, Y. F. Xi, J. X. Zhu, G. Q. Zhu and H. P. He, *Appl. Catal., B*, 2019, **255**, 117739.
45 Y. Dai, C. Xu, X. Sun and X. Chen, *Chem. Soc. Rev.*, 2017, **46**, 3830–3852.
46 T. P. Szatrowski and C. F. Nathan, *Cancer Res.*, 1991, **51**, 794–798.
47 J. Kim, H. R. Cho, H. Jeon, D. Kim, C. Song, N. Lee, S. H. Choi and T. Hyeon, *J. Am. Chem. Soc.*, 2017, **139**, 10992–10995.
48 Y. S. Jung, W. T. Lim, J. Y. Park and Y. H. Kim, *Environ. Technol.*, 2009, **30**, 183–190.
49 A. D. Bokare and W. Choi, *J. Hazard. Mater.*, 2014, **275**, 121–135.
50 W. Feng, X. Han, R. Wang, X. Gao, P. Hu, W. Yue, Y. Chen and J. Shi, *Adv. Mater.*, 2019, **31**, 1805919.
51 S. Gao, H. Lin, H. Zhang, H. Yao, Y. Chen and J. Shi, *Adv. Sci.*, 2019, **6**, 1801733.
52 S. Gao, X. Lu, P. Zhu, H. Lin, L. Yu, H. Yao, C. Wei, Y. Chen and J. Shi, *J. Mater. Chem. B*, 2019, **7**, 3599–3609.
53 L. Feng, R. Xie, C. Wang, S. Gai, F. He, D. Yang, P. Yang and J. Lin, *ACS Nano*, 2018, **12**, 11000–11012.
54 Z. Tang, H. Zhang, Y. Liu, D. Ni, H. Zhang, J. Zhang, Z. Yao, M. He, J. Shi and W. Bu, *Adv. Mater.*, 2017, **29**, 1701683.
55 Z. Cao, L. Zhang, K. Liang, S. Cheong, C. Boyer, J. J. Gooding, Y. Chen and Z. Gu, *Adv. Sci.*, 2018, **5**, 1801155.
56 Y. Liu, P. C. Naha, G. Hwang, D. Kim, Y. Huang, A. Simon-Soro, H.-I. Jung, Z. Ren, Y. Li, S. Gubara, F. Alawi, D. Zero, A. T. Hara, D. P. Cormode and H. Koo, *Nat. Commun.*, 2018, **9**, 2920.
57 P. C. Naha, Y. Liu, G. Hwang, Y. Huang, S. Gubara, V. Jonnakuti, A. Simon-Soro, D. Kim, L. Gao, H. Koo and D. P. Cormode, *ACS Nano*, 2019, **13**, 4960–4971.
58 L. Gao, Y. Liu, D. Kim, Y. Li, G. Hwang, P. C. Naha, D. P. Cormode and H. Koo, *Biomaterials*, 2016, **101**, 272–284.
59 H. Zhao, Y. Wang, Y. Wang, T. Cao and G. Zhao, *Appl. Catal., B*, 2012, **125**, 120–127.
60 N. Masomboon, C. Ratanatamskul and M.-C. Lu, *Environ. Sci. Technol.*, 2009, **43**, 8629–8634.
61 V. Poza-Nogueiras, E. Rosales, M. Pazos and M. Angeles Sanroman, *Chemosphere*, 2018, **201**, 399–416.
62 L. Lyu, L. L. Zhang and C. Hu, *Chem. Eng. J.*, 2015, **274**, 298–306.
63 D. A. Nichela, A. M. Berkovic, M. R. Costante, M. P. Juliarena and F. S. G. Einschlag, *Chem. Eng. J.*, 2013, **228**, 1148–1157.
64 A. N. Pham, A. L. Rose and T. D. Waite, *J. Phys. Chem. A*, 2012, **116**, 6590–6599.
65 E. Brillas, M. A. Banos, S. Camps, C. Arias, P. L. Cabot, J. A. Garrido and R. M. Rodriguez, *New J. Chem.*, 2004, **28**, 314–322.
66 T. Soltani and B.-K. Lee, *Chem. Eng. J.*, 2017, **313**, 1258–1268.
67 T. D. Rae, P. J. Schmidt, R. A. Pufahl, V. C. Culotta and T. V. O'Halloran, *Science*, 1999, **284**, 805–808.
68 K. Jomova and M. Valko, *Toxicology*, 2011, **283**, 65–87.
69 N. Verma and N. Kumar, *ACS Biomater. Sci. Eng.*, 2019, **5**, 1170–1188.
70 P. Szymanski, T. Fraczek, M. Markowicz and E. Mikiciuk-Olasik, *Biometals*, 2012, **25**, 1089–1112.
71 B. Ma, S. Wang, F. Liu, S. Zhang, J. Duan, Z. Li, Y. Kong, Y. Sang, H. Liu, W. Bu and L. Li, *J. Am. Chem. Soc.*, 2019, **141**, 849–857.
72 L.-S. Lin, T. Huang, J. Song, X.-Y. Ou, Z. Wang, H. Deng, R. Tian, Y. Liu, J.-F. Wang, Y. Liu, G. Yu, Z. Zhou, S. Wang, G. Niu, H.-H. Yang and X. Chen, *J. Am. Chem. Soc.*, 2019, **141**, 9937–9945.
73 H. J. Kim, K. H. Min, H. J. Lee, Y.-S. Hwang and S. C. Lee, *J. Ind. Eng. Chem.*, 2019, DOI: 10.1016/j.jiec.2019.07.004.
74 X. Liu, Z. Yan, Y. Zhang, Z. Liu, Y. Sun, J. Ren and X. Qu, *ACS Nano*, 2019, **13**, 5222–5230.
75 C. Zhang, L. Yan, X. Wang, X. Dong, R. Zhou, Z. Gu and Y. Zhao, *Nano Lett.*, 2019, **19**, 1749–1757.
76 R. Hu, Y. Fang, M. Huo, H. Yao, C. Wang, Y. Chen and R. Wu, *Biomaterials*, 2019, **206**, 101–114.
77 X. Wang, X. Zhong, H. Lei, Y. Geng, Q. Zhao, F. Gong, Z. Yang, Z. Dong, Z. Liu and L. Cheng, *Chem. Mater.*, 2019, **31**, 6174–6186.
78 T. Li, J. Zhou, L. Wang, H. Zhang, C. Song, J. M. de la Fuente, Y. Pan, J. Song, C. Zhang and D. Cui, *Adv. Healthcare Mater.*, 2019, **8**, 1900192.
79 S. Goel, F. Chen and W. Cai, *Small*, 2014, **10**, 631–645.
80 Q. W. Tian, M. H. Tang, Y. G. Sun, R. J. Zou, Z. G. Chen, M. F. Zhu, S. P. Yang, J. L. Wang, J. H. Wang and J. Q. Hu, *Adv. Mater.*, 2011, **23**, 3542–3547.
81 M. Zhou, R. Zhang, M. A. Huang, W. Lu, S. L. Song, M. P. Melancon, M. Tian, D. Liang and C. Li, *J. Am. Chem. Soc.*, 2010, **132**, 15351–15358.
82 L. R. Guo, D. D. Yan, D. F. Yang, Y. J. Li, X. D. Wang, O. Zalewski, B. F. Yan and W. Lu, *ACS Nano*, 2014, **8**, 5670–5681.
83 X. Yi, K. Yang, C. Liang, X. Y. Zhong, P. Ning, G. S. Song, D. L. Wang, C. C. Ge, C. Y. Chen, Z. F. Chai and Z. Liu, *Adv. Funct. Mater.*, 2015, **25**, 4689–4699.
84 L. Dong, K. Li, D. Wen, Y. Lu, K. Du, M. Zhang, X. Gao, J. Feng and H. Zhang, *Nanoscale*, 2019, **11**, 12853–12857.
85 W. Wu, L. Yu, Q. Jiang, M. Huo, H. Lin, L. Wang, Y. Chen and J. Shi, *J. Am. Chem. Soc.*, 2019, **141**, 11531–11539.
86 X. Peng, Q. Pan, B. Zhang, S. Wan, S. Li, K. Luo, Y. Pu and B. He, *Biomacromolecules*, 2019, **20**, 2372–2383.
87 P. E. Tawari, Z. P. Wang, M. Najlah, C. W. Tsang, V. Kannappan, P. Liu, C. McConville, B. He, A. L. Armesilla and W. G. Wang, *Toxicol. Res.*, 2015, **4**, 1439–1442.
88 Z. Skrott, M. Mistrik, K. K. Andersen, S. Friis, D. Majera, J. Gursky, T. Ozdian, J. Bartkova, Z. Turi, P. Moudry, M. Kraus, M. Michalova, J. Vaclavkova, P. Dzubak, I. Vrobel, P. Pouckova, J. Sedlacek, A. Miklovicova, A. Kutt, J. Li, J. Mattova, C. Driessen, Q. P. Dou, J. Olsen, M. Hajduch, B. Cvek, R. J. Deshaies and J. Bartek, *Nature*, 2017, **552**, 194–199.

89 D. J. Lewis, P. Deshmukh, A. A. Tedstone, F. Tuna and P. O'Brien, *Chem. Commun.*, 2014, **50**, 13334–13337.
90 C. Conticello, D. Martinetti, L. Adamo, S. Buccheri, R. Giuffrida, N. Parrinello, L. Lombardo, G. Anastasi, G. Amato, M. Cavalli, A. Chiarenza, R. De Maria, R. Giustolisi, M. Gulisano and F. Di Raimondo, *Int. J. Cancer*, 2012, **131**, 2197–2203.
91 D. Z. Cen, D. Brayton, B. Shahandeh, F. L. Meyskens and P. J. Farmer, *J. Med. Chem.*, 2004, **47**, 6914–6920.
92 C.-G. Liu, Y.-H. Han, J.-T. Zhang, R. K. Kankala, S.-B. Wang and A.-Z. Chen, *Chem. Eng. J.*, 2019, **370**, 1188–1199.
93 X. Cai, Z. Xie, B. Ding, S. Shao, S. Liang, M. Pang and J. Lin, *Adv. Sci.*, 2019, **6**, 1900848.
94 E. Ju, K. Dong, Z. Chen, Z. Liu, C. Liu, Y. Huang, Z. Wang, F. Pu, J. Ren and X. Qu, *Angew. Chem., Int. Ed.*, 2016, **55**, 11467–11471.
95 C. Wang, F. Cao, Y. Ruan, X. Jia, W. Zhen and X. Jiang, *Angew. Chem., Int. Ed.*, 2019, **58**, 9846–9850.
96 K. Ni, T. Aung, S. Li, N. Fatuzzo, X. Liang and W. Lin, *Chem*, 2019, **5**, 1892–1913.
97 Y. Yang, J. Tang, P. L. Abbaraju, M. Jambhrunkar, H. Song, M. Zhang, C. Lei, J. Fu, Z. Gu, Y. Liu and C. Yu, *Angew. Chem., Int. Ed.*, 2018, **57**, 11764–11769.
98 C. Wang, L. Xu, C. Liang, J. Xiang, R. Peng and Z. Liu, *Adv. Mater.*, 2014, **26**, 8154–8162.
99 Q. Chen, L. Xu, C. Liang, C. Wang, R. Peng and Z. Liu, *Nat. Commun.*, 2016, **7**, 13193.
100 C. He, X. Duan, N. Guo, C. Chan, C. Poon, R. R. Weichselbaum and W. Lin, *Nat. Commun.*, 2016, **7**, 12499.
101 G. Yang, L. Xu, Y. Chao, J. Xu, X. Sun, Y. Wu, R. Peng and Z. Liu, *Nat. Commun.*, 2017, **8**, 902.
102 B. Li, Z. Gu, N. Kurniawan, W. Chen and Z. P. Xu, *Adv. Mater.*, 2017, **29**, 1700373.
103 T. Kim, E. J. Cho, Y. Chae, M. Kim, A. Oh, J. Jin, E. S. Lee, H. Baik, S. Haam, J. S. Suh, Y. M. Huh and K. Lee, *Angew. Chem., Int. Ed.*, 2011, **50**, 10589–10593.
104 L. Yu, Y. Chen, M. Wu, X. Cai, H. Yao, L. Zhang, H. Chen and J. Shi, *J. Am. Chem. Soc.*, 2016, **138**, 9881–9894.
105 Z. P. Zhen and J. Xie, *Theranostics*, 2012, **2**, 45–54.
106 J. M. Shin, R. M. Anisur, M. K. Ko, G. H. Im, J. H. Lee and I. S. Lee, *Angew. Chem., Int. Ed.*, 2009, **48**, 321–324.
107 J. Lu, S. Ma, J. Sun, C. Xia, C. Liu, Z. Wang, X. Zhao, F. Gao, Q. Gong, B. Song, X. Shuai, H. Ai and Z. Gu, *Biomaterials*, 2009, **30**, 2919–2928.
108 H. Fan, Z. Zhao, G. Yan, X. Zhang, C. Yang, H. Meng, Z. Chen, H. Liu and W. Tan, *Angew. Chem., Int. Ed.*, 2015, **127**, 4883–4887.
109 S. Wang, F. Li, R. Qiao, X. Hu, H. Liao, L. Chen, J. Wu, H. Wu, M. Zhao, J. Liu, R. Chen, X. Ma, D. Kim, J. Sun, T. P. Davis, C. Chen, J. Tian, T. Hyeon and D. Ling, *ACS Nano*, 2018, **12**, 12380–12392.
110 Z. Liu, S. Zhang, H. Lin, M. Zhao, H. Yao, L. Zhang, W. Peng and Y. Chen, *Biomaterials*, 2018, **155**, 54–63.
111 M. Song, T. Liu, C. Shi, X. Zhang and X. Chen, *ACS Nano*, 2016, **10**, 633–647.
112 T. S. Lin, X. Z. Zhao, S. Zhao, H. Yu, W. M. Cao, W. Chen, H. Wei and H. Q. Guo, *Theranostics*, 2018, **8**, 990–1004.
113 J. T. Xu, W. Han, P. P. Yang, T. Jia, S. M. Dong, H. T. Bi, A. Gulzar, D. Yang, S. L. Gai, F. He, J. Lin and C. X. Li, *Adv. Funct. Mater.*, 2018, **28**, 1803804.
114 Q. Chen, L. Feng, J. Liu, W. Zhu, Z. Dong, Y. Wu and Z. Liu, *Adv. Mater.*, 2016, **28**, 7129–7136.
115 L. T. Meng, Y. L. Cheng, X. N. Tong, S. J. Gan, Y. W. Ding, Y. Zhang, C. Wang, L. Xu, Y. S. Zhu, J. H. Wu, Y. Q. Hu and A. Yuan, *ACS Nano*, 2018, **12**, 8308–8322.
116 W. Fan, W. Bu, B. Shen, Q. He, Z. Cui, Y. Liu, X. Zheng, K. Zhao and J. Shi, *Adv. Mater.*, 2015, **27**, 4155–4161.
117 L.-S. Lin, J. Song, L. Song, K. Ke, Y. Liu, Z. Zhou, Z. Shen, J. Li, Z. Yang, W. Tang, G. Niu, H.-H. Yang and X. Chen, *Angew. Chem., Int. Ed.*, 2018, **57**, 4902–4906.
118 C. Liu, D. Wang, S. Zhang, Y. Cheng, F. Yang, Y. Xing, T. Xu, H. Dong and X. Zhang, *ACS Nano*, 2019, **13**, 4267–4277.
119 B. Ding, S. Shao, F. Jiang, P. Dang, C. Sun, S. Huang, P. A. Ma, D. Jin, A. A. Al Kheraif and J. Lin, *Chem. Mater.*, 2019, **31**, 2651–2660.
120 M. Orecchioni, R. Cabizza, A. Bianco and L. G. Delogu, *Theranostics*, 2015, **5**, 710–723.
121 K. Yang, L. Z. Feng and Z. Liu, *Adv. Drug Delivery Rev.*, 2016, **105**, 228–241.
122 L. Y. Feng, L. Wu and X. G. Qu, *Adv. Mater.*, 2013, **25**, 168–186.
123 O. Akhavan and E. Ghaderi, *ACS Nano*, 2010, **4**, 5731–5736.
124 S. B. Liu, T. H. Zeng, M. Hofmann, E. Burcombe, J. Wei, R. R. Jiang, J. Kong and Y. Chen, *ACS Nano*, 2011, **5**, 6971–6980.
125 W. B. Hu, C. Peng, W. J. Luo, M. Lv, X. M. Li, D. Li, Q. Huang and C. H. Fan, *ACS Nano*, 2010, **4**, 4317–4323.
126 Y. Tu, M. Lv, P. Xiu, T. Huynh, M. Zhang, M. Castelli, Z. Liu, Q. Huang, C. Fan, H. Fang and R. Zhou, *Nat. Nanotechnol.*, 2013, **8**, 594–601.
127 D. W. Park, A. A. Schendel, S. Mikael, S. K. Brodnick, T. J. Richner, J. P. Ness, M. R. Hayat, F. Atry, S. T. Frye, R. Pashaie, S. Thongpang, Z. Q. Ma and J. C. Williams, *Nat. Commun.*, 2014, **5**, 15258.
128 J. Joo, E. J. Kwon, J. Y. Kang, M. Skalak, E. J. Anglin, A. P. Mann, E. Ruoslahti, S. N. Bhatia and M. J. Sailor, *Nanoscale Horiz.*, 2016, **1**, 407–414.
129 C. J. Wan, L. Q. Zhu, Y. H. Liu, P. Feng, Z. P. Liu, H. L. Cao, P. Xiao, Y. Shi and Q. Wan, *Adv. Mater.*, 2016, **28**, 3557–3563.
130 B. Ling, H. Chen, D. Liang, W. Lin, X. Qi, H. Liu and X. Deng, *ACS Appl. Mater. Interfaces*, 2019, **11**, 11157–11166.
131 K. Fan, J. Xi, L. Fan, P. Wang, C. Zhu, Y. Tang, X. Xu, M. Liang, B. Jiang, X. Yan and L. Gao, *Nat. Commun.*, 2018, **9**, 1440.
132 Y. Hu, X. J. Gao, Y. Zhu, F. Muhammad, S. Tan, W. Cao, S. Lin, Z. Jin, X. Gao and H. Wei, *Chem. Mater.*, 2018, **30**, 6431–6439.
133 S. Lin, Y. Zhang, W. Cao, X. Wang, L. Qin, M. Zhou and H. Wei, *Dalton Trans.*, 2019, **48**, 1993–1999.
134 Q. Wu, G. Wei, Z. Xu, J. Han, J. Xi, L. Fan and L. Gao, *ACS Appl. Mater. Interfaces*, 2018, **10**, 25026–25036.

135 J. Xi, G. Wei, Q. Wu, Z. Xu, Y. Liu, J. Han, L. Fan and L. Gao, *Biomater. Sci.*, 2019, DOI: 10.1039/c9bm00705a.
136 J. R. Morones, J. L. Elechiguerra, A. Camacho, K. Holt, J. B. Kouri, J. T. Ramirez and M. J. Yacaman, *Nanotechnology*, 2005, **16**, 2346–2353.
137 S. Chernousova and M. Epple, *Angew. Chem., Int. Ed.*, 2013, **52**, 1636–1653.
138 I. Sondi and B. Salopek-Sondi, *J. Colloid Interface Sci.*, 2004, **275**, 177–182.
139 M. Rai, A. Yadav and A. Gade, *Biotechnol. Adv.*, 2009, **27**, 76–83.
140 V. K. Sharma, R. A. Yngard and Y. Lin, *Adv. Colloid Interface Sci.*, 2009, **145**, 83–96.
141 E. Boisselier and D. Astruc, *Chem. Soc. Rev.*, 2009, **38**, 1759–1782.
142 X. H. Huang, S. Neretina and M. A. El-Sayed, *Adv. Mater.*, 2009, **21**, 4880–4910.
143 M. S. Yavuz, Y. Y. Cheng, J. Y. Chen, C. M. Cobley, Q. Zhang, M. Rycenga, J. W. Xie, C. Kim, K. H. Song, A. G. Schwartz, L. H. V. Wang and Y. N. Xia, *Nat. Mater.*, 2009, **8**, 935–939.
144 S. E. Skrabalak, J. Y. Chen, Y. G. Sun, X. M. Lu, L. Au, C. M. Cobley and Y. N. Xia, *Acc. Chem. Res.*, 2008, **41**, 1587–1595.
145 L. C. Kennedy, L. R. Bickford, N. A. Lewinski, A. J. Coughlin, Y. Hu, E. S. Day, J. L. West and R. A. Drezek, *Small*, 2011, **7**, 169–183.
146 S. Tang, M. Chen and N. Zheng, *Small*, 2014, **10**, 3139–3144.
147 W. J. Fang, S. H. Tang, P. X. Liu, X. L. Fang, J. W. Gong and N. F. Zheng, *Small*, 2012, **8**, 3816–3822.
148 X. M. Zhu, H. Y. Wan, H. L. Jia, L. Liu and J. F. Wang, *Adv. Healthcare Mater.*, 2016, **5**, 3165–3172.
149 P. P. Xu, H. H. Wu, D. D. Wang, G. Z. Zhao, F. F. Li, B. S. Qiu, Z. Guo and Q. W. Chen, *Adv. Healthcare Mater.*, 2018, **7**, 1800322.
150 W. L. Wang, Z. X. Guo, Y. Lu, X. C. Shen, T. Chen, R. T. Huang, B. Zhou, C. C. Wen, H. Liang and B. P. Jiang, *ACS Appl. Mater. Interfaces*, 2019, **11**, 17294–17305.
151 L.-Y. Duan, Y.-J. Wang, J.-W. Liu, Y.-M. Wang, N. Li and J.-H. Jiang, *Chem. Commun.*, 2018, **54**, 8214–8217.
152 W.-L. Wang, Z. Guo, Y. Lu, X.-C. Shen, T. Chen, R.-T. Huang, B. Zhou, C. Wen, H. Liang and B.-P. Jiang, *ACS Appl. Mater. Interfaces*, 2019, **11**, 17294–17305.
153 Z. Ma, L. Wu, K. Han and H. Han, *Nanoscale Horiz.*, 2019, **4**, 1124–1131.
154 H. Song, Z. Li, Y. Peng, X. Li, X. Xu, J. Pan and X. Niu, *Analyst*, 2019, **144**, 2416–2422.
155 Z. Wang, Y. Zhang, E. Ju, Z. Liu, F. Cao, Z. Chen, J. Ren and X. Qu, *Nat. Commun.*, 2018, **9**, 3334.
156 A. Zhang, S. Pan, Y. Zhang, J. Chang, J. Cheng, Z. Huang, T. Li, C. Zhang, J. Martinez de la Fuentea, Q. Zhang and D. Cui, *Theranostics*, 2019, **9**, 3443–3458.
157 P. Liu, Y. Wang, L. An, Q. Tian, J. Lin and S. Yang, *ACS Appl. Mater. Interfaces*, 2018, **10**, 38833–38844.
158 Y. Liu, Q. Jia, Q. Guo, W. Wei and J. Zhou, *Biomaterials*, 2018, **180**, 104–116.
159 L. Wen, L. Chen, S. M. Zheng, J. F. Zeng, G. X. Duan, Y. Wang, G. L. Wang, Z. F. Chai, Z. Li and M. Y. Gao, *Adv. Mater.*, 2016, **28**, 5072–5079.
160 J. J. Qiu, Q. F. Xiao, X. P. Zheng, L. B. Zhang, H. Y. Xing, D. L. Ni, Y. Y. Liu, S. J. Zhang, Q. G. Ren, Y. Q. Hua, K. L. Zhao and W. B. Bu, *Nano Res.*, 2015, **8**, 3580–3590.
161 Z. G. Chen, Q. Wang, H. L. Wang, L. S. Zhang, G. S. Song, L. L. Song, J. Q. Hu, H. Z. Wang, J. S. Liu, M. F. Zhu and D. Y. Zhao, *Adv. Mater.*, 2013, **25**, 2095–2100.
162 Z. Liu, F. Wang, J. Ren and X. Qu, *Biomaterials*, 2019, **208**, 21–31.
163 T. Jia, J. Xu, S. Dong, F. He, C. Zhong, G. Yang, H. Bi, M. Xu, Y. Hu, D. Yang, P. Yang and J. Lin, *Chem. Sci.*, 2019, DOI: 10.1039/C9SC01615E.
164 F. Cao, Y. Zhang, Y. Sun, Z. Wang, L. Zhang, Y. Huang, C. Liu, Z. Liu, J. Ren and X. Qu, *Chem. Mater.*, 2018, **30**, 7831–7839.
165 J. Niu, Y. Sun, F. Wang, C. Zhao, J. Ren and X. Qu, *Chem. Mater.*, 2018, **30**, 7027–7033.
166 X. Wang, C. Zhang, J. Du, X. Dong, S. Jian, L. Yan, Z. Gu and Y. Zhao, *ACS Nano*, 2019, **13**, 5947–5958.